Spin Foams, Refinement Limit,

自旋泡沫、精化极限,

and Renormalization

与重整化

Contents

目录

Abstract

摘要

Spin foams provide path integrals for quantum gravity, which employ dis-cretizations as regulator. To obtain regulator independent predictions, we must remove these fiducial structures in a suitable refinement limit. In this chapter we present the current state of research: we begin with a discussion on the role of diffeomorphism symmetries in discrete systems, the notion of scale in background independent theories, and how we can consistently improve theories via renormalization to reduce regulator dependence. We present the consistent boundary formulation, which provides a renormalization framework for background independent theories, and discuss tensor network methods and restricted spin foams, which provide concrete renormalization algorithms aiming at the construction of consistent boundary amplitudes for spin foams. We furthermore discuss effective spin foams, which have allowed for the construction of a perturbative refinement limit and an associated effective continuum action.

自旋泡沫为量子引力提供了路径积分，该理论将离散化用作正则化。为了得到与正则化无关的预言，我们必须在合适的精修极限中移除这些基准结构。本章我们介绍该领域的研究现状: 我们首先讨论微分同胚对称性在离散系统中的作用、背景无关理论中的标度概念，以及我们如何通过重整化一致改进理论，以降低对正则化的依赖。我们介绍了为背景无关理论提供重整化框架的一致边界表述，还讨论了张量网络方法与受限自旋泡沫，这些方法给出了具体的重整化算法，旨在构造自旋泡沫的一致边界振幅。我们进一步讨论了有效自旋泡沫，该理论已经允许构造微扰精修极限以及对应的有效连续作用量。

S. K. Asante ·S. Steinhaus

S. K. 阿桑特·S. 施泰因豪斯

Theoretisch-Physikalisches Institut, Friedrich-Schiller-Universität Jena, Jena, Germany e-mail: seth.asante@uni-jena.de; sebastian.steinhaus@uni-jena.de

德国耶拿市弗里德里希-席勒耶拿大学理论物理研究所电子邮箱:seth.asante@uni-jena.de; sebastian.steinhaus@uni-jena.de

B. Dittrich (☑)

B. 迪特里希 (☑)

Perimeter Institute for Theoretical Physics, Waterloo, ON, Canada

加拿大安大略省滑铁卢市圆周理论物理研究所

e-mail: bdittrich@perimeterinsitute.ca; bdittrich@perimeterinstitute.ca

电子邮箱:bdittrich@perimeterinsitute.ca; bdittrich@perimeterinstitute.ca

---

Keywords

关键词

Quantum gravity - Spin foams · Regge calculus · Renormalization · Numerical methods · Tensor networks

量子引力-自旋泡沫 · 里奇微积分 · 重整化 · 数值方法 · 张量网络

Introduction

引言

Spin foams construct non-perturbative path integrals for quantum gravity, which implement a rigorous notion of quantum geometry. Such path integrals require however a regularization, which for spin foams is implemented via a discretization.

自旋泡沫构建了量子引力的非微扰路径积分，实现了严格的量子几何概念。但这类路径积分需要正则化，自旋泡沫的正则化通过离散化实现。

This regulator has to be removed in order to obtain sensible amplitudes, which do not depend on arbitrary discretization choices. That is, we have to determine the refinement limit. This can be implemented via renormalization algorithms, which organize this enormous computational challenge into iterative steps and allow for truncation schemes.

必须移除该正则化因子才能得到不依赖任意离散化选择的合理振幅，也就是说，我们需要确定精化极限。这可以通过重整化算法实现，该算法将这项庞大的计算难题拆分为迭代步骤，并允许使用截断方案。

This chapter is organized as follows:

本章结构安排如下:

Section ”Basics of Regge Calculus and Spin Foams:” provides some basic background on Regge calculus and spin foams needed for the following discussions.

“里奇微积分与自旋泡沫基础”一节: 提供后续讨论所需的里奇微积分与自旋泡沫基础背景知识。

Section ”The Need for Renormalization: Restoring Diffeomorphism Symmetry:” discusses why constructing the refinement limit is indispensable in order to restore diffeomorphism symmetry and to obtain discretization independent amplitudes.

“重整化的必要性: 恢复微分同胚对称性”一节: 讨论为何构建精化极限对于恢复微分同胚对称性、得到不依赖离散化的振幅是必不可少的。

Section ”The Notion of Scale and Renormalization Flow of Couplings in Diffeomorphism Invariant Systems:” explains how to define a notion of scale and renormalization flow of couplings for background independent theories such as spin foams.

“微分同胚不变系统中的标度概念与耦合常数重整化流”一节: 讲解如何为自旋泡沫这类背景无关理论定义标度概念与耦合常数重整化流。

Section ”The Consistent Boundary Formalism:” sketches the consistent boundary formalism. This provides a framework to construct and express the refinement limit via a family of consistent amplitudes for spacetime regions with finer and finer boundary data. The consistency conditions motivate an iterative renormalization scheme, applicable to background independent theories and preserving the locality of (spin foam) amplitudes.

“一致性边界形式”一节: 概述一致性边界形式。该形式提供了一个框架，通过为边界数据越来越精细的时空区域构造一族一致振幅来构建并表示精化极限。一致性条件催生了适用于背景无关理论、且能保持 (自旋泡沫) 振幅局域性的迭代重整化方案。

Section ”Tensor Network Renormalization:” discusses tensor network algorithms and their adaption and application to (analogue) spin foams. Tensor network algorithms can be understood as realizing the construction of consistent boundary amplitudes.

“张量网络重整化”一节: 讨论张量网络算法及其对 (类比) 自旋泡沫的适配与应用。张量网络算法可被理解为实现了一致性边界振幅的构造。

Section ”Restricted Spin Foam Models:” discusses the renormalization flow of restricted spin foams, which arises from a combination of symmetry reduction and semi-classical approximation from the full spin foam models.

“受限自旋泡沫模型”一节: 讨论受限自旋泡沫的重整化流，这类模型源自完整自旋泡沫模型的对称性约化与半经典近似结合。

Section ”Effective Spin Foam Models and Their Refinement Limit:” sketches effective spin foam models and first results on their (perturbative) refinement limit.

“有效自旋泡沫模型及其精化极限”一节: 概述有效自旋泡沫模型，以及其 (微扰) 精化极限的初步结果。

Section ”Concluding Remarks:” provides a short summary and comments on some open issues.

“结语”一节: 提供简短总结，并对若干开放问题做了评述。

Basics of Regge Calculus and Spin Foams

里奇微积分与自旋泡沫基础

Here we will introduce basic facts and notions of Regge calculus and spin foams.

这里我们将介绍里奇微积分与自旋泡沫的基本事实和概念。

Regge calculus [1] is a discretization of general relativity, defined on triangulations. Its fundamental degrees of freedom are the edge lengths of the triangulation. It is a coordinate-free theory, as we only refer to the distances between vertices, not how these vertices are embedded. The basic building blocks of a d -dimensional triangulation are d -simplices, which are defined as the convex hull of $(d+1)$ vectors in $\mathbb{R}^d$ (or $\mathbb{R}^{(1,d-1)}$ for Lorentzian signature). So, d -simplices can be embedded into d -dimensional flat spacetime and are thus intrinsically flat. A simplex is uniquely described (up to translations, rotations, etc.) by its edge lengths, e.g., six edge lengths for a 3-simplex (tetrahedron) or ten edge lengths for a 4-simplex. From the edge lengths of a simplex, we compute its dihedral angles, i.e., the angles enclosed between two $(d-1)$ -simplices. The angle is associated with the $(d-2)$ -simplex shared by the $(d-1)$ -simplices. Curvature in Regge calculus is

distributional and encoded in deficit angles associated with $(d-2)$ -simplices, e.g., triangles in 4D. A deficit angle measures the difference between 2π and the sum of dihedral angles of d -simplices that contain the $(d-2)$ -simplex. The dynamics of the theory is encoded in the Regge action, which is a discretization of the Einstein-Hilbert action.

里奇微积分 [1] 是定义在三角剖分上的广义相对论离散化形式，其基本自由度是三角剖分的边长。它是一个无坐标理论，因为我们仅涉及顶点之间的距离，不涉及这些顶点如何嵌入。d 维三角剖分的基本构造块是 d 单形，定义为 $(d+1)$ 个向量在 $\mathbb{R}^d$ 中的凸包 (洛伦兹号差时为 $\mathbb{R}^{(1,d-1)}$)。因此 d 单形可以嵌入 d 维平坦时空，本身是内禀平坦的。一个单形 (除平移、旋转等变换外) 可由其边长唯一描述，例如 3 单形 (四面体) 有 6 个边长，4 单形有 10 个边长。我们可以从单形的边长计算其二面角，即两个 $(d-1)$ 单形之间的夹角。该角度与两个 $(d-1)$ 单形共有的 $(d-2)$ 单形相关联。里奇微积分中的曲率是分布性的，编码在与 $(d-2)$ 单形相关的亏缺角中，例如四维情况下亏缺角对应三角形。亏缺角衡量 2π 与所有包含该 $(d-2)$ 单形的 d 单形的二面角之和的差值。该理论的动力学由里奇作用量编码，里奇作用量是爱因斯坦-希尔伯特作用量的离散化形式。

Area Regge calculus [2], on the other hand, is a 4D theory that uses areas of triangles instead of edge lengths as its fundamental variables. The 4-simplices are again intrinsically flat and determined by the values of its ten triangle areas, i.e., the deficit angles are functions of these areas. While the number of triangles is the same as the number of edges in a 4-simplex, for larger triangulations we have (generically) much more triangles than edges. To formulate a theory in terms of area variables equivalent to (length) Regge calculus, additional constraints must be imposed [3].

另一方面，面积里奇微积分 [2] 是一个四维理论，它使用三角形面积而非边长作为基本变量。4 单形仍然是内禀平坦的，由其 10 个三角形的面积值确定，即亏缺角是这些面积的函数。虽然单个 4 单形中三角形的数量与边的数量相等，但对于更大的三角剖分，一般来说三角形的数量远多于边的数量。要构造一个与 (边长) 里奇微积分等价的面积变量理论，必须引入额外约束 [3]。

Spin foams [4, 5] are path integrals for quantum gravity, defined on a 2-complex. This 2-complex is frequently chosen to be dual to a triangulation. It consists of vertices, edges, and faces. Vertices are dual to d -simplices, edges are dual to $(d-1)$ -simplices, and faces are dual to $(d-2)$ -simplices. The 2-complex is colored with group (The groups in questions are SO(4) for Euclidean signature models and $\mathrm{SO}(3,1)$ for Lorentzian signature models.) theoretic data, which are quantum numbers encoding geometry. In 4D, irreducible representations of the group, associated with the faces, encode their areas, whereas tensors invariant under the action of the group, called intertwiners, are assigned to edges. They encode the shape of 3D polyhedra [6]. A spin foam model then locally assigns amplitudes to the 2-complex: vertex amplitudes to vertices, edge amplitudes to edges, and face amplitudes to faces. These amplitudes are derived from general relativity expressed as a constrained topological quantum field theory [7]. A frequently derived result elucidates [8-11] the connection of spin foams to (Area) Regge calculus: in the limit where all representations are large, the spin foam vertex amplitude is dominated by boundary data corresponding to geometric 4-simplices, and it oscillates with the Regge action associated with the 4-simplex.

自旋泡沫 [4,5] 是定义在 2 复形上的量子引力路径积分。这个 2 复形通常被选为三角剖分的对偶。它由顶点、边和面组成: 顶点对偶于 d 单形，边对偶于 $(d-1)$ 单形，面对偶于 $(d-2)$ 单形。2 复形带有群论数据标记 (涉及的群对欧几里得号差模型是 SO(4)，对洛伦兹号差模型是 $\mathrm{SO}(3,1)$)，这些数据是编码几何信息的量子数。在四维中，与面对应的群不可约表示编码面的面积，而分配给边的是群作用下不变的张量，称为缠绕元，编码三维多面体的形状 [6]。自旋泡沫模型对 2 复形局域地分配振幅: 顶点分配顶点振幅，边分配边振幅，面分配面振幅。这些振幅由表述为约束拓扑量子场论的广义相对论导出 [7]。一个得到广泛认可的结果阐明了自旋泡沫与 (面积) 里奇微积分之间的联系 [8-11]: 当所有表示都很大时，自旋泡沫顶点振幅由对应几何 4 单形的边界数据主导，其振荡行为由该 4 单形对应的里奇作用量描述。

The Need for Renormalization: Restoring Diffeomorphism Symmetry

重整化的必要性: 恢复微分同胚对称性

The spin foam approach, much like Regge calculus, is based on a discretization of the underlying spacetime manifold. Such discretizations do often interfere with diffeomorphism symmetry.

自旋泡沫方法与里奇微积分非常相似，都基于 underlying 时空流形的离散化。这类离散化通常会破坏微分同胚对称性。

The question whether Regge gravity features diffeomorphism symmetry has been debated in the literature [12-15]. On the one hand, diffeomorphisms have been identified in linearized Regge gravity around a flat background [12]. Here the diffeomorphism modes are essential to obtain the correct number of two propagating graviton modes in the continuum limit. Arguments have been put forward [12,14] that the existence of such gauge symmetries should extend to the full theory. On the other hand, the data associated with Regge triangulations do not include any obvious notion of embedding coordinates (We will see below that this is similar to time reparametrization invariant systems, where the auxiliary time parameter also does not appear in the description of the discrete dynamics.), on which diffeomorphisms could act. Therefore it has been often suggested that each distinct Regge configuration defines a distinct geometry. Furthermore, Regge solutions with curvature are typically uniquely specified by their boundary data, which speaks against the existence of gauge symmetries.

里奇引力是否具有微分同胚对称性，这一问题已有文献争论 [12-15]。一方面，人们已在平坦背景下的线性化里奇引力中识别出微分同胚 [12]。在此，微分同胚模对于在连续极限中得到正确数量的两个传播引力子模至关重要。已有论证 [12,14] 指出，这类规范对称性应当可以拓展至整个理论。另一方面，与里奇三角剖分相关的数据并不包含任何明显的嵌入坐标概念 (我们在下文中会看到，这与时间重新参数化不变系统类似，这类系统的辅助时间参数也不会出现在离散动力学的描述中)，而微分同胚需要作用在嵌入坐标上。因此人们通常认为，每个不同的里奇构型对应一个不同的几何。此外，带曲率的里奇解通常由其边界数据唯一确定，这也不支持规范对称性的存在。

This debate arose due to the common, but in this context misleading, characterization of gauge symmetries as (local) transformations acting on the dynamical variables, which leave the action invariant [14]. Requiring invariance of the action constitutes only one condition on the action. An action with N variables admits, locally around each point with non-vanishing gradient, $(N-1)$ such transformations.

这场争论的起源是: 一种常见但在该语境下具有误导性的观点将规范对称性定义为作用在动力学变量上、保持作用量不变的 (局部) 变换 [14]。要求作用量不变仅对作用量提出了一个条件。一个具有 N 变量的作用量，在每个梯度非零的点附近局部容许 $(N-1)$ 个这类变换。

Most of these transformations act, however, trivially on configurations that define solutions of the system [16, 17]. In fact, whether gauge symmetries have a nontrivial action or not does depend on the given solution. In the case of Regge gravity (without cosmological constant), flat solutions do feature gauge symmetries, whereas solutions with curvature typically do not.

但大多数这类变换对定义系统解的构型的作用是平凡的 [16, 17]。实际上，规范对称性是否具有非平凡作用，依赖于具体给定的解。在 (无宇宙学常数的) 里奇引力中，平坦解确实具有规范对称性，而带曲率的解通常不具有。

It is indeed advantageous to think of 4D (In 3D Regge gravity (without cosmological constant), all solutions are flat, and diffeomorphism symmetry is not broken.)

将 4 维 (在 3 维里奇引力 (无宇宙学常数) 中，所有解都是平坦的，微分同胚对称性不会破缺。)

Regge gravity as having broken diffeomorphisms [16-18]. This can be turned into a quantitative statement: if there is a non-trivial action of a gauge symmetry on a given solution, then the Hessian of the action, evaluated on this solution, has null modes, that is, vanishing eigenvalues. Broken symmetries are characterized by nonvanishing eigenvalues, whose absolute values are much smaller than the absolute values of the remaining eigenvalues.

里奇引力视为微分同胚破缺的理论确实更方便 [16-18]。这可以转化为一个定量表述: 如果规范对称性在给定解上存在非平凡作用，那么在该解上计算得到的作用量的海森矩阵存在零模，也就是本征值为零。破缺的对称性的特征是海森矩阵具有非零本征值，且这些本征值的绝对值远小于其余本征值的绝对值。

4D Regge gravity solutions with curvature [17], 3D Regge gravity solutions with cosmological constant [16], as well as area Regge solutions with non-metricity [18] all feature broken diffeomorphism symmetries in this sense.

带曲率的 4 维里奇引力解 [17]、带宇宙学常数的 3 维里奇引力解 [16]，以及带非度规性的面积里奇解 [18]，在这个意义下都具有破缺的微分同胚对称性。

The same concepts apply to simple mechanical systems: by adding time t to the configuration variables q^B , one can introduce reparametrizations as a gauge symmetry. Starting from a Lagrangian $L\left(q^B, dq^B/dt\right)$, we define a new Lagrangian

同样的概念也适用于简单力学系统: 通过在构型变量 q^B 中引入时间 t ，我们可以将重新参数化作为一种规范对称性引入。从拉格朗日量 $L\left(q^B, dq^B/dt\right)$ 出发，我们定义新的拉格朗日量

$$L_{ri}\left(q^B, dq^B/ds, t, dt/ds\right) = L\left(q, \frac{dq^B/ds}{dt/ds}\right) dt/ds, \tag{1}$$

with an auxiliary parameter s. The action $\int_{s_0}^{s_1} L_{ri} ds$ along a path $(q(s), t(s))$ is invariant, if we apply a reparametrization $(q(f(s)), t(f(s)))$, where f is a monotonic function with $f(s_0) = s_0$ and $f(s_1) = s_1$. This holds for all paths, including solutions; we have therefore a gauge symmetry.

其中带有辅助参数 s。沿路径 $(q(s), t(s))$ 的作用量 $\int_{s_0}^{s_1} L_{ri} ds$ 在我们应用重新参数化 $(q(f(s)), t(f(s)))$ 时保持不变，其中 f 是满足 $f(s_0) = s_0$ 和 $f(s_1) = s_1$ 的单调函数。这对所有路径都成立，包括解；因此我们得到了一个规范对称性。

Discretizing such systems typically breaks reparametrization symmetry [19,20]. This can only be avoided by perfect discretizations [19,21].

对这类系统进行离散化通常会破坏重新参数化对称性 [19,20]。只有完美离散化才能避免这一点 [19,21]。

Such perfect (This notion is inspired by perfect actions developed for Lattice QCD [22].) discretizations are defined to exactly mirror continuum dynamics [20, 23]: given a map from the set of variables in the discretization to continuum observables, a discretization is said to be perfect, if the discrete solutions do agree with the continuum solutions, as probed by the observables.

这类完美 (这个概念的灵感来自格点量子色动力学中发展出的完美作用量 [22]。) 离散化被定义为精确反映连续动力学 [20, 23]: 给定一个从离散化变量集合到连续可观测量的映射，如果离散解与可观测量探测到的连续解完全一致，那么这个离散化就是完美的。

For mechanical systems, the classical perfect action, that is, the action describing a perfect discretization, agrees with the Hamilton-Jacobi function, aka Hamilton's principal function [19,21,23].

对于力学系统，经典完美作用量 (即描述完美离散化的作用量) 与哈密顿-雅可比函数 (也叫哈密顿主函数) 一致 [19,21,23]。

That is, consider a dynamical system with time parameter (We allow here systems with and without reparametrization invariance. For the latter s can be identified with t, for the former t is part of the variables, e.g., $x^0 = t$.) s and variables x^A. The dynamics is described by a Lagrangian $L_C\left(x^A, \dot{x}^A\right)$, where $\dot{x}^A$ is dx^A/ds. The Hamilton-Jacobi function is defined as action evaluated on solutions, that is,

也就是说，考虑一个带时间参数的动力学系统 (我们这里同时允许具有和不具有重参数化不变性的系统，对于后者 s 可以等同于 t，对于前者 t 是变量的一部分，例如 $x^0 = t$。)，有 s 和变量 x^A。动力学由拉格朗日量 $L_C\left(x^A, \dot{x}^A\right)$ 描述，其中 $\dot{x}^A$ 为 dx^A/ds。哈密顿-雅可比函数定义为作用量在解上的求值，即:

$$S_{HJ}\left(x_1^A, s_1; x_0^A, s_0\right) = \int L_C\left(x_{|sol}^A(s), \dot{x}_{|sol}^A(s)\right) \mathrm{d}s, \tag{2}$$

where $x_{|sol}^A$ extremizes the action, with $x_{|sol}^A(s_0) = x_0^A$ and $x_{|sol}^A(s_1) = x_1^A$. From this definition follows the following important additivity property:

其中 $x^A_{|\mathrm{sol}}$ 使作用量取极值，满足 $x^A_{|\mathrm{sol}}(s_0) = x^A_0$ 和 $x^A_{|\mathrm{sol}}(s_1) = x^A_1$。根据该定义可得到下述重要可加性:

$$S_{\mathrm{HJ}}\left(x^A_1, s_1; x^A_0, s_0\right) = \mathrm{Ext}_{x^A_z}\left(S_{\mathrm{HJ}}\left(x^A_1, s_1; x^A_z, s_z\right) + S_{\mathrm{HJ}}\left(x^A_z, s_z; x^A_0, s_0\right)\right). \tag{3}$$

Here $\mathrm{Extr}_{x^A_z} F\left(x^A_z\right)$ means that we take the extremum of F over the range of $\left\{x^A_z\right\}_A$. Note that this extremum is attained at $x^A_{|\mathrm{sol}}(s_z)$, that is, the solution evaluated at s_z.

此处 $\mathrm{Extr}_{x^A_z} F\left(x^A_z\right)$ 表示我们对 F 在 $\left\{x^A_z\right\}_A$ 的取值范围内取极值。注意该极值在 $x^A_{|\mathrm{sol}}(s_z)$ 处取得，也就是解在 s_z 处的求值。

The action for a perfect discretization is given by

完美离散化的作用量由下式给出:

$$S_{\mathrm{Per}}\left(\left\{x^A_n\right\}\right) = \sum_{n=0}^{N-1} S_{\mathrm{HJ}}\left(x^A_{n+1}, s_{n+1}; x^A_n, s_n\right). \tag{4}$$

Here $\{s_n\}_{n=0}^N$ are discrete time values and $\left\{x^A_n\right\}_A$ the corresponding set of variables at time parameter s_n. This perfect action reproduces the continuum dynamics: Given boundary values $\left(x^A_0, s_0\right)$ and $\left(x^A_N, s_N\right)$, the extremum of the discrete action is given by $x^A_n = x^A_{|\,\mathrm{sol}\,|}(s_n)$, where $x^A_{|\,\mathrm{sol}\,|}(s)$ is the continuum solution [21].

此处 $\{s_n\}_{n=0}^N$ 是离散时间值，$\left\{x^A_n\right\}_A$ 是时间参数 s_n 处对应的变量集合。该完美作用量可以重现连续介质动力学: 给定边界值 $\left(x^A_0, s_0\right)$ 和 $\left(x^A_N, s_N\right)$，离散作用量的极值由 $x^A_n = x^A_{|\,\mathrm{sol}\,|}(s_n)$ 给出，其中 $x^A_{|\,\mathrm{sol}\,|}(s)$ 是连续介质解 [21]。

With the perfect mirroring of the continuum dynamics, one expects that symmetries of the continuum action, that can be captured by the discrete variables, are present for the perfect discretization.

由于完美离散化可以完全复刻连续介质动力学，我们因此可以预期，连续介质作用量中可被离散变量捕捉到的对称性，在完美离散化中也依然存在。

Indeed, consider a continuum action with time reparameterization invariance. Instead of unique solutions $x^A_{|\mathrm{sol}}(s)$, we have families of solutions $x^A_{|\mathrm{sol}}(f(s))$ with monotonic functions f. The perfect action (4) will lead to a mirroring of this behavior: an entire family of solutions is given by $x^A_n = x^A_{|\mathrm{sol}}(f(s_n))$.

事实上，考虑具有时间重参数化不变性的连续介质作用量。我们得到的不是唯一解 $x^A_{|\mathrm{sol}}(s)$，而是带单调函数 f 的解族 $x^A_{|\mathrm{sol}}(f(s))$。完美作用量 (4) 会复刻这一行为: 整个解族由 $x^A_n = x^A_{|\mathrm{sol}}(f(s_n))$ 给出。

The perfect action (4) shows also a notion of discretization independence: the perfect action (4) evaluated on a solution with fixed boundary values $\left(x^A_{\mathrm{in}}, s_{\mathrm{in}}\right) = \left(x^A_0, s_0\right), \left(x^A_{\mathrm{out}}, s_{\mathrm{out}}\right) = \left(x^A_N, s_N\right)$ does not depend on the number of subdivided points. It is always given by the continuum Hamilton-Jacobi function.

完美作用量 (4) 还表现出离散化无关性: 在固定边界值 $\left(x^A_{\text{in}}, s_{\text{in}}\right) = \left(x^A_0, s_0\right), \left(x^A_{\text{out}}, s_{\text{out}}\right) = \left(x^A_N, s_N\right)$ 的解上求值时，完美作用量 (4) 不依赖于细分点的数量，它始终等于连续介质的哈密顿-雅可比函数。

Thus, the perfect action (4) is also a fixed point of the following refinement (We use here refinement flow instead of the more widely used term coarse graining flow, as we first refine and then solve for the degrees of freedom added by the refinement. We will discuss in section "The Notion of Scale and Renormalization Flow of Couplings in Diffeomorphism Invariant Systems" the notion of scale in more detail.) flow: starting from a discrete action $S_{\text{D}}\left(x^A_1, s_1; x^A_0, s_0\right)$ for a time interval, we subdivide this interval into two and compute a new action

因此，完美作用量 (4) 也是下述精修流的不动点 (此处我们使用精修流而非更通用的粗粒化流术语，原因是我们先进行精修，再求解精修引入的自由度。我们会在"微分同胚不变系统中的标度概念与重整化流耦合"章节更详细地讨论标度概念): 从一个时间区间的离散作用量 $S_{\text{D}}\left(x^A_1, s_1; x^A_0, s_0\right)$ 出发，我们将该区间细分为两段，计算得到一个新作用量

$$S'_{\text{D}}\left(x^A_1, s_1; x^A_0, s_0\right) = \text{Extr}_{x^A_z}\left(S_{\text{D}}\left(x^A_1, s_1; x^A_z, s_z\right) + S_{\text{D}}\left(x^A_z, s_z; x^A_0, s_0\right)\right). \tag{5}$$

The additivity property (3) of the Hamilton-Jacobi function ensures that the perfect action (4) is invariant under this flow, $S'_{\text{Per}} = S_{\text{Per}}$.

哈密顿-雅可比函数的可加性 (3) 保证了完美作用量 (4) 在该流之下不变，$S'_{\text{Per}} = S_{\text{Per}}$ 。

This suggest two ways to calculate a perfect discretization: (a) one can solve the continuum dynamics and compute the Hamilton-Jacobi function, which defines the perfect action. This blocking from the continuum [24-26] might, however, be only practical for free theories. Another possibility is to start with a discrete action and subject it to the refinement flow (5). Alternatively, one can solve the corresponding fixed point conditions. The latter method allows to find analytical expressions for perfect actions also in the case of more complicated systems [20,26].

这给出了两种计算完美离散化的方法:(a) 可以求解连续动力学并计算哈密顿-雅可比函数，由此定义完美作用量。不过这种从连续出发的分块方法 [24-26] 可能仅适用于自由理论。另一种方法是从离散作用量出发，令其经受精修流 (5)，也可以求解对应的不动点条件。后一种方法 even 对于更复杂系统也能得到完美作用量的解析表达式 [20,26]。

The notion of perfect discretization and refinement flow applies also to the quantum case [20, 26] . The role of the Hamilton-Jacobi function is taken over by the quantum mechanical propagator

完美离散化和精修流的概念也适用于量子情形 [20, 26] 。此时量子力学传播子取代了哈密顿-雅可比函数的角色

$$K\left(x^A_1, s_1; x^A_0, s_0\right) = \left\langle x^A_1, s_1 \mid x^A_0, s_0 \right\rangle. \tag{6}$$

The additivity property (3) translates into the convolution property for the (continuum) propagator K_{C}

可加性 (3) 转化为 (连续) 传播子的卷积性质 K_{C}

$$K_{\mathrm{C}}\left(x_1^A, s_1; x_0^A, s_0\right) = \int K_{\mathrm{C}}\left(x_1^A, s_1; x_z^A, s_z\right) K_{\mathrm{C}}\left(x_z^A, s_z; x_0^A, s_0\right) \prod_A \mathrm{d}x_z^A. \tag{7}$$

We can define a quantum version of the refinement flow (5), given by

我们可以定义精修流 (5) 的量子版本，由下式给出

$$K'_{\mathrm{D}}\left(x_1^A, s_1; x_0^A, s_0\right) = \int K_{\mathrm{D}}\left(x_1^A, s_1; x_z^A, s_z\right) K_{\mathrm{D}}\left(x_z^A, s_z; x_0^A, s_0\right) \prod_A \mathrm{d}x_z^A, \tag{8}$$

where K_{D} is a discretization of the quantum amplitude. The convolution property (7) of the continuum amplitude K_{C} ensures that it is a fixed point of the flow defined by (8). Such fixed points can be obtained by applying (8) iteratively or by directly solving the fixed point conditions. The latter method allows to construct propagators [20] and has been used to determine one-loop measures for the path integral [26].

其中 K_{D} 是量子振幅的一种离散化。连续振幅 K_{C} 的卷积性质 (7) 保证了它是 (8) 所定义流的不动点。这类不动点可以通过迭代应用 (8) 得到，也可以直接求解不动点条件得到。后一种方法可以构造传播子 [20]，已被用于确定路径积分的单圈测度 [26]。

We so far assumed systems with or without reparametrization invariance. If the continuum system has reparametrization invariance, then the Hamilton-Jacobi function (2) and the propagator (6) will not depend on the auxiliary time parameter values s_0 and s_1 . Such systems can be discretized such that the action and propagator will not depend on the s -values, even if this discretization is not perfect.

到目前为止，我们讨论的系统包含或不包含重参数化不变性都成立。如果连续系统具有重参数化不变性，那么哈密顿-雅可比函数 (2) 和传播子 (6) 都不依赖于辅助时间参数值 s_0 和 s_1 。我们可以对这类系统进行离散化，使得作用量和传播子都不依赖于 s 值，即便该离散化不是完美的。

Consider, for example, a reparametrization invariant system, describing a particle in a potential, with variables $x^0 = t, x^1 = q$. The continuum action is given by

举个例子，考虑一个描述势场中粒子的重参数化不变系统，其变量为 $x^0 = t, x^1 = q$ 。连续作用量由下式给出

$$S_{\mathrm{C}} = \int ds \left(\frac{1}{2}\dot{q}^2 (\dot{t})^{-1} - V(q)\,\dot{t}\right), \tag{9}$$

which can be discretized to

可以将其离散化为

$$S_{\mathrm{D}} = \sum_{n=0}^{N-1} \frac{1}{2}\left((q_{n+1} - q_n)^2 (t_{n+1} - t_n)^{-1} - \frac{1}{2}\left(V(q_{n+1}) + V(q_n)\right)(t_{n+1} - t_n)\right). \tag{10}$$

The reparametrization invariance is typically (The symmetry is not broken for vanishing potential, as with the discretization (10) the particle trajectory is piecewise linear and the free particle trajectory is linear in (t, q) space.) broken by the discretization, i.e., fixing boundary values (q_N, t_N, q_0, t_0) , the solutions for the q_n and t_n are unique.

重参数化不变性通常 (零势下该对称性不会破缺, 因为在离散化 (10) 下粒子轨迹是分段线性的, 而自由粒子轨迹在 (t,q) 空间中本身就是线性的) 会被离散化破缺，也就是说，固定边界值 (q_N,t_N,q_0,t_0) 后，q_n 和 t_n 的解是唯一的。

The s -parameter can be understood as auxiliary time coordinate. Its nonappearance for discretizations of reparametrization invariant systems is analogous to the non-appearance of spacetime coordinates in Regge calculus. We showed that there is nevertheless a notion of (broken) reparametrization symmetry for these systems. The same holds for (broken) diffeomorphisms in the case of Regge calculus.

s 参数可以理解为辅助时间坐标。它在重参数化不变系统离散化中不出现，类比于时空坐标在里奇微积分中不出现。我们已经证明，这些系统仍然存在 (破缺的) 重参数化对称性这一概念。对于里奇微积分中 (破缺的) 微分同胚，情况也是如此。

Similar concepts apply to the discretizations of field theories. There is however a key difference between systems based on one-dimensional spacetime and higher-dimensional systems. The refinement flow in one-dimensional systems with local (Here we mean with local actions and amplitudes which only couple variables associated with top-dimensional building blocks.) actions preserves this locality. This does not apply for higher-dimensional systems.

类似的概念也适用于场论的离散化。但一维时空系统和高维系统之间存在一个关键区别: 对于一维系统，具有局域性 (此处我们指局域作用量和振幅仅耦合最高维积木所关联的变量) 的作用量，其精修流会保持该局域性。这一点对高维系统不成立。

The heuristic reason for this is the following: one-dimensional systems are often discretized by subdividing the one-dimensional spacetime into edges. The ”amount” of boundary data is the same for one edge and for a gluing of a number of edges into a ”refined” edge; see Fig. 1. The finer data, which are integrated out for the refinement flow, all reside inside the refined edge. The refinement does therefore not introduce couplings between the data associated with different refined edges.

其启发式原因如下: 一维系统通常通过将一维时空细分为边来离散化。一条边与多条边胶合而成的“细边”所拥有的边界数据“量”是相同的；参见图 1。为粗化流积分掉的更精细数据全部位于细边内部。因此，粗化不会在不同细边关联的数据之间引入耦合。

For higher-dimensional systems, however, the amount of boundary data increases, when refining building blocks; see Fig. 1. In many refinement schemes one therefore coarse grains the boundary data of the refined blocks, that is, subdivides these data into a coarse set and a fine set and integrates out all the finer data. As these finer data on the boundary are shared by at least two refined blocks, this does generically lead to couplings between these blocks. With each refinement iteration the couplings then connect blocks that are farther and farther apart.

然而，对于高维系统，粗化构造块时边界数据量会增加；参见图 1。因此在许多粗化方案中，会对粗化块的边界数据做粗粒化处理，即将这些数据分为粗数据集和细数据集，然后积分掉所有更精细的数据。由于边界上的这些精细数据至少由两个粗化块共享，这通常会导致这些块之间产生耦合。每一次粗化迭代后，耦合会连接越来越远的块。

We will discuss in section ”The Consistent Boundary Formalism” refinement schemes, which avoid this

mechanism of producing nonlocal couplings. This happens by introducing a truncation for the boundary data of the refined building blocks. Here it will be crucial to carefully choose the truncation: in fact, it should be adapted to the dynamics of the system.

我们将在“一致边界形式”一节讨论避免这种非局部耦合产生机制的粗化方案，该方案通过对粗化构造块的边界数据引入截断实现。此处谨慎选择截断至关重要: 实际上，截断需要适配系统的动力学。

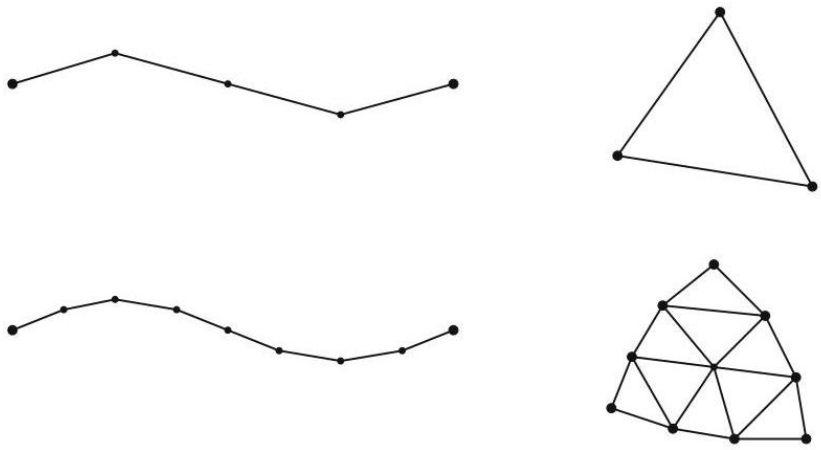

Fig. 1 Left: Under refinement of a one-dimensional discrete system, the boundary data remains unchanged. Right: For higher dimensions, refining the discretization implies a refinement of the boundary. For example, for a discretized scalar field, a triangular building block built from nine ”smaller” triangles carries more boundary data than the smaller triangles

图 1 左: 一维离散系统粗化后，边界数据保持不变。右: 对于高维，离散化粗化意味着边界的粗化。例如，对于离散标量场，由九个“更小”三角形构成的三角形构造块，携带的边界数据比小三角形更多

One example, where improved and perfect actions have been constructed, is Regge gravity with cosmological constant [23]. In particular the 3D action based on homogeneously curved building blocks is perfect, as the solutions are also homogeneously curved. This provides an example where the broken diffeomorphism invariance of 3D Regge gravity with cosmological constant is regained via a refinement procedure.

已经构造出改进作用量和完美作用量的一个例子是带宇宙学常数的里奇引力 [23]。特别是基于均匀弯曲构造块的三维作用量是完美的，因为其解也是均匀弯曲的。这提供了一个例子: 带宇宙学常数的三维里奇引力破缺的微分同胚不变性可以通过粗化过程恢复。

Perfect actions have been also constructed for lattice QCD [24] and for linearized field theories with gauge symmetries, including electromagnetism as well as 3D and 4D gravity [25, 26]. The choice of how to coarse grain the fields should respect the gauge symmetries [25], but there is still quite some freedom, which can influence how nonlocal the resulting action is [27]. One can also import the notion of perfect action into the Hamiltonian framework and construct ”perfect Hamiltonians” [28-31].

完美作用量也已经在格点量子色动力学 [24] 和带规范对称性的线性化场论中构造出来，包括电磁学以及三维和四维引力 [25, 26]。场的粗粒化方式选择需要尊重规范对称性 [25]，但仍存在相当多的自由度，这会影响最终作用量的非局域程度 [27]。也可以将完美作用量的概念引入哈密顿框架，构造“完美哈密顿量”[28-31]。

Perfect amplitudes have been constructed to one-loop order for the anharmonic oscillator, for 3D Regge gravity, as well as for linearized 4D gravity [20, 26, 32]. In fact, solving the fixed point equations derived from (7) leads to an alternative construction for the continuum path integral. It can in particular be used to determine the path integral measure [26, 32, 33] .

完美振幅已经在非简谐振子、三维里奇引力以及线性化四维引力的单圈阶构造完成 [20, 26, 32]。实际上，求解从 (7) 导出的不动点方程可以得到连续路径积分的另一种构造方式，它特别可以用于确定路径积分测度 [26, 32, 33] 。

Restoring diffeomorphism invariance comes with further advantages:

恢复微分同胚不变性还有更多优点:

- Discrete systems with diffeomorphism invariance are also discretization independent and thus perfect [20, 34]. For example, choosing discretizations with different number of building blocks leads to the same predictions.

  - 具有微分同胚不变性的离散系统也不依赖于离散化，因此是完美的 [20, 34]。例如，选择构造块数量不同的离散化会得到相同的预言。

- In constructing discrete actions and amplitudes, one faces lots of ambiguities. As systems with diffeomorphism invariance are perfect, and thus at a fixed point of the coarse graining flow, these ambiguities are usually resolved. The work [20] proofed that such ambiguities disappear for a class of one-dimensional systems.

  - 在构造离散作用量和振幅时，会存在大量歧义。由于具有微分同胚不变性的系统是完美的，即处于粗粒化流的不动点，这些歧义通常会被消除。文献 [20] 证明，对于一类一维系统，这类歧义都会消失。

- Restoring diffeomorphism invariance means that one can properly split the variables into physical observables and gauge degrees of freedom. One can also define a canonical formalism for discrete (time) systems [35-39]. If diffeomorphism invariance is not broken, one will obtain constraints, which are first class [40,41]. This does allow to derive a consistent discretization of Hamiltonian systems with diffeomorphism symmetry. Correspondingly a (discretized) path integral with diffeomorphism symmetry will act as a projector onto the wave functions satisfying the constraints [20,42].

  - 恢复微分同胚不变性意味着可以将变量正确拆分为物理可观测量和规范自由度。还可以为离散 (时间) 系统定义正则形式 [35-39]。如果微分同胚不变性没有破缺，我们将得到第一类约束 [40,41]。这使得我们可以导出具有微分同胚对称性的哈密顿系统的一致离散化。相应地，具有微分同胚对称性的 (离散化) 路径积分会投影到满足约束的波函数上 [20,42]。

In contrast, for systems, where diffeomorphism symmetry is broken, one has pseudo-constraints [35, 36, 40] . These are equations of motions, which depend very weakly on some variables - the pseudo gauge variables. Although one could argue that the ”problem of implementing the constraints for initial data” has disappeared, choosing the initial data freely will typically result in solutions with unphysical properties [16, 35, 36] .

反之，对于微分同胚对称性破缺的系统，会存在伪约束 [35, 36, 40] 。这些是运动方程，它们对某些变量 (伪规范变量) 的依赖极弱。尽管有人可能会说“对初始数据施加约束的问题”已经消失，但自由选择初始数据通常会得到具有非物理性质的解 [16, 35, 36] 。

- Broken diffeomorphism symmetry leads to inconsistencies for perturbation theory. These can be resolved in a framework where diffeomorphism symmetry and discretization independence are restored order by order [34].

- 破缺的微分同胚对称性会导致微扰理论出现不自洽性，这些问题可以在逐阶恢复微分同胚对称性和离散化无关性的框架中解决 [34]。

The first point implies that restoring diffeomorphism invariance is equivalent to having full control over the solutions of the system. Gravity being nonlinear, we can only hope for a truncation scheme. Often it is already helpful to obtain improved amplitudes, which deliver discretization independent results for coarse observables. We will discuss in section ”The Consistent Boundary Formalism” a renormalization scheme for the construction of consistent amplitudes, which (a) preserve the locality of amplitudes and (b) implement a refinement flow and (c) a truncation adapted to the dynamics of the system.

第一点意味着恢复微分同胚不变性等价于完全掌握该系统的所有解。由于引力是非线性的，我们只能寄希望于截断方案。通常，获取改进振幅就已经很有帮助了，这类振幅能给出粗粒可观测量的离散化无关结果。我们将在“一致边界形式”一节讨论一种用于构造一致振幅的重整化方案，该方案 (a) 保留振幅的局域性，(b) 实现粗化流，(c) 采用适配系统动力学的截断。

The Notion of Scale and Renormalization Flow of Couplings in Diffeomorphism Invariant Systems

微分同胚不变系统中的标度概念与耦合常数重整化流

Here we discuss the notion of scale and how the flow of coupling constants is realized in diffeomorphism invariant systems. Although coarse graining/refinement algorithms for such systems will be very similar to, e.g., condensed matter systems, it is important to note the differences in interpreting the results.

我们在此讨论微分同胚不变系统中的标度概念，以及耦合常数流如何实现。尽管这类系统的粗粒化/细化算法与凝聚态系统等非常相似，但必须注意结果诠释上的差异。

For condensed matter systems, one assumes initial amplitudes at a fixed small scale, referred to as lattice constant. Usually these amplitudes are seen as fundamental description, from which one derives effective amplitudes to describe the dynamics at larger scales. To this end, one applies coarse graining, i.e., starting

from the fundamental lattice, one coarse grains the fundamental building blocks into larger blocks and correspondingly fundamental variables into coarser observables. One then integrates out finer degrees of freedom, obtaining in this way an effective dynamics for the coarser observables at a larger lattice scale. This process can be iterated, producing effective dynamics at different lattice scales.

对于凝聚态系统，人们假设初始振幅定义在固定小标度，即晶格常数。通常这些振幅被视为基础描述，我们由此推导出有效振幅来描述更大标度的动力学。为此我们引入粗粒化: 从基础晶格出发，将基础结构单元粗化为更大的块，相应地将基础变量转化为更粗的可观测量。随后积分掉更精细的自由度，由此得到更大晶格标度下粗可观测量的有效动力学。这个过程可以迭代，得到不同晶格标度下的有效动力学。

Often, one can describe these effective dynamics via effective actions, and these can be parameterized via coupling constants. That is, the effective dynamics at different lattice scales is described by effective actions having the same form, but with different values of the coupling constants. This defines a "renormalization flow of the coupling constants," i.e., these are functions of the lattice scale.

通常，这些有效动力学可以通过有效作用量描述，并且可以用耦合常数参数化。也就是说，不同晶格标度下的有效动力学由形式相同但耦合常数值不同的有效作用量描述。这就定义了“耦合常数的重整化流”，即耦合常数是晶格标度的函数。

For diffeomorphism invariant systems, the situation is different: the initial amplitudes describe a discrete system, which can have arbitrary scale. "Scale" or the "lattice constant" are part of the basic variables. A possible measure for scale in the discretization of the reparametrization invariant system (10) is given by the differences $(t_{n+1} - t_n)$. As these are part of the dynamical variables, one needs to solve the dynamics in order to determine their values (The solution will generally lead to values for the $(t_{n+1} - t_n)$, which differ for different n . That is, the lattice constant should be rather understood to be a function of (space-)time.), But the average size is determined by $(t_N - t_0)/N$, and this size can be chosen - via the boundary data - to be arbitrarily small or arbitrarily large. This is a general property of diffeomorphism invariant systems: the lattice scale is determined by the boundary data and the number of building blocks used in the discretization.

对于微分同胚不变系统，情况有所不同: 初始振幅描述的离散系统可具有任意标度。“标度”或“晶格常数”本身就是基本变量的一部分。重参数化不变系统 (10) 离散化后，一种可行的标度度量由差值 $(t_{n+1} - t_n)$ 给出。由于这些差值属于动力学变量，我们需要求解动力学才能确定它们的值 (求解后通常会得到 $(t_{n+1} - t_n)$ 的数值，不同 n 对应的数值各不相同，也就是说晶格常数更应当被理解为 (空间) 时间的函数)。但其平均尺寸由 $(t_N - t_0)/N$ 决定，并且该尺寸可通过边界数据任意调大或调小。这是微分同胚不变系统的普遍性质: 晶格标度由边界数据和离散化所用构造块的数量决定。

If the lattice scale is large, the discrete actions provide typically bad approximations to the continuum dynamics. For example, (10) gives only a good approximation to the continuum dynamics, if $|V(q_{n+1}) - V(q_n)| \ll |q_{n+1} - q_n|^2/|t_{n+1} - t_n|^2$. Therefore, we do not interpret a given discretization of a diffeomorphism invariant system, which breaks this symmetry, as fundamental. Rather, it serves as an approximation to the dynamics defined by the perfect action.

若晶格标度较大，离散作用通常只能对连续动力学给出很差的近似。例如，只有当 $|V(q_{n+1}) - V(q_n)| \ll |q_{n+1} - q_n|^2/|t_{n+1} - t_n|^2$ 时，(10) 才能对连续动力学给出良好近似。因此，我们并不把破坏了对称性的既定微分同胚不变系统离散化视为基础性内容，相反，它仅用作完美作用定义动力学的一种近似。

Different from the condensed matter case, we therefore see the refinement procedure (5) as a process of improving this approximation. One can extract from this refinement procedure a notion of flowing coupling constants, but this rather reflects the process of constructing better and better approximations to the perfect action.

因此与凝聚态情况不同，我们将细化过程 (5) 视为改进这种近似的过程。我们可以从这个细化过程中得到流动耦合常数的概念，但这更多反映了我们不断构造对完美作用量更好近似的过程。

This improvement of the dynamics affects in particular the action for larger scales. For example, the harmonic oscillator action can be discretized as

动力学的这种改进尤其会影响大标度下的作用量。例如，简谐振子作用量可以离散化为:

$$S_{\mathrm{D}} = \sum_{n=0}^{N-1} \frac{1}{2}\left((q_{n+1} - q_n)^2 (t_{n+1} - t_n)^{-1} - \frac{\omega^2}{2}\left(q_{n+1}^2 + q_n^2\right)(t_{n+1} - t_n)\right). \tag{11}$$

The corresponding perfect action is given by [20]

对应的完美作用量由文献 [20] 给出

$$S_{\mathrm{Per}} = \sum_{n=0}^{N-1} \frac{\omega}{2} \frac{\left(\cos\left(\omega\left(t_{n+1} - t_n\right)\right)\left(q_{n+1}^2 + q_n^2\right) - 2q_{n+1}q_n\right)}{\sin\left(\omega\left(t_{n+1} - t_n\right)\right)}. \tag{12}$$

S_{D} does approximate well S_{Per} for $\omega\left(t_{n+1} - t_n\right) \ll 1$, but not for $\omega\left(t_{n+1} - t_n\right) > 1$.

S_{D} 在 $\omega(t_{n+1} - t_n) \ll 1$ 情况下可以很好地近似 S_{Per} ，但在 $\omega(t_{n+1} - t_n) > 1$ 情况下不行。

The fixed point action (12) does describe a consistent dynamics, valid over all scales: the dynamics at larger scales can be obtained either from probing the action directly at larger scales (as set by the boundary data and number of building blocks) or by probing the action at smaller scales but computing only coarse observables. For a perfect action these two different procedures give the same result.

不动点作用量 (12) 确实描述了适用于所有标度的自洽动力学: 大标度下的动力学既可以直接在大标度 (由边界数据和结构单元数量设定) 下探测作用量得到，也可以在小标度下探测作用量、仅计算粗可观测量得到。对于完美作用量，这两种不同过程会给出相同的结果。

Thus, the perfect action does encode the dynamics of all scales at once and therefore also the renormalization flow of the coupling constants. For example, for (12), we declared $(t_{n+1} - t_n)$ as representing a notion of lattice scale. The perfect action is a quadratic polynomial in (q_{n+1}, q_n) . The coupling constants can be defined to be given by the corresponding coefficients, which are functions depending on $(t_{n+1} - t_n)$.

These coupling constants are therefore functions of the lattice scale, given by the differences $(t_{n+1} - t_n)$. This dependence represents a physically relevant notion of renormalization flow of coupling constants.

因此，完美作用量确实同时编码了所有能标的动力学，因此也包含了耦合常数的重整化流。例如，对于式 (12)，我们将 $(t_{n+1} - t_n)$ 定义为格点能标概念的表示。完美作用量是 (q_{n+1}, q_n) 上的二次多项式。耦合常数可定义为对应的系数，这些系数是依赖于 $(t_{n+1} - t_n)$ 的函数。因此这些耦合常数都是格点能标的函数，由差值 $(t_{n+1} - t_n)$ 给出。这种依赖关系就是物理上相关的耦合常数重整化流概念。

For diffeomorphism invariant systems, such as gravity, the scale is given in terms of the spacetime metric. For reparametrization invariant field systems, one does add the spacetime coordinates as variables, and a spacetime metric can be introduced as function of these coordinates. Thus the notion of "running couplings" translates into couplings which are functionals depending on the spacetime metric.

对于微分同胚不变系统 (例如引力)，能标由时空度量给出。对于重参数化不变场系统，我们会将时空坐标添加为变量，并且可以将时空度量作为这些坐标的函数引入。因此，“跑动耦合”的概念就转化为依赖于时空度量的泛函形式的耦合。

In section "The Need for Renormalization: Restoring Diffeomorphism Symmetry" we mentioned that one can also determine the perfect action by solving the fixed point conditions for the iterative refinement procedure (10). These fixed point conditions constitute equations for the coupling constants as functions of the $(t_{n+1} - t_n)$; see [20]. Solving these equations is analogous to solving the flow equations for the coupling constants, e.g., in the asymptotic safety approach [43]. In solving the fixed point conditions, one does not necessarily need to produce a solution by determining the coupling constants for larger scales from smaller scales. In principle one can also determine the smaller scales from larger scales. As in the asymptotic safety program [43], we expect this to be relevant for quantum gravity, where one rather knows the IR dynamics and is looking for an UV completion.

在“对重整化的需求: 恢复微分同胚对称性”一节中，我们提到过也可以通过迭代细化过程 (10) 求解不动点条件来确定完美作用量。这些不动点条件构成了耦合常数作为 $(t_{n+1} - t_n)$ 函数的方程，参见文献 [20]。求解这些方程类似于求解耦合常数的流方程，例如渐近安全方法中的情形 [43]。求解不动点条件时，不一定需要从小能标出发确定大能标的耦合来得到解。原则上也可以从大能标出发确定小能标。和渐近安全项目 [43] 一样，我们预计这对量子引力是有意义的——量子引力中我们更多是已知红外动力学，寻找紫外完备。

We have seen that for reparametrization invariant systems, the renormalization flow of coupling constants appears in a different guise as compared to usual lattice systems. This does not mean that we can avoid the need to fine-tune couplings in the initial discrete amplitudes. Finding the fixed points (i.e., perfect amplitudes) via the refinement procedure (8) does require to take infinitely many iteration steps. Without fine-tuning the infinite iterations might lead to divergent amplitudes or end up in trivial fixed points. Indeed even for quantum mechanical systems, one does need to fine-tune parameters describing the path integral measure [20, 26, 44] .

我们已经看到，对于重参数化不变系统，耦合常数的重整化流表现形式与普通格点系统不同。这不意味着我们可以免去对初始离散振幅中的耦合进行精细调节。通过细化过程 (8) 寻找不动点 (即完美振幅) 确实需要无穷多迭代步骤。不进行精细调节的话，无穷迭代可能会导致振幅发散，或者最终落到平庸不动点上。事实上即便是量子力学系统，也需要对描述路径积分测度 [20, 26, 44] 的参数进行精细调节。

Although there is a large difference in the way lattice constants and flow of coupling constants appear in systems with and without diffeomorphism invariance, the actual coarse graining algorithms, e.g., the tensor network algorithms discussed in section "Tensor Network Renormalization," are often the same.

尽管在有无微分同胚不变性的系统中，格点常数和耦合常数流的存在方式存在很大差异，但实际的粗粒化算法往往是相同的，例如“张量网络重整化”一节讨论的张量网络算法。

As a final note, we stress again that the "refinement limit," as implemented by the refinement flows (5), (8) for diffeomorphism invariant systems, should be seen as an auxiliary construction to obtain a perfect discretization. For such systems quantities like "scale" are part of the dynamical variables; we therefore do not send a lattice constant to zero. In loop quantum gravity and spin foams, observables which can be used to identify a scale, like areas and volumes, do have a discrete spectrum in the quantum theory [45], with a minimal non-vanishing eigenvalue. This physical notion of discreteness is expected to be preserved under the refinement limit [46].

最后我们再次强调，针对微分同胚不变系统由细化流 (5)、(8) 实现的“细化极限”，应当被视为获得完美离散化的辅助构造。在这类系统中，“能标”这类量本身就是动力学变量的一部分；因此我们不需要将格点常数取为零。在圈量子引力和自旋泡沫中，可用于确定能标的可观测量 (例如面积和体积) 在量子理论中具有离散谱 [45]，且存在最小非零本征值。这种物理上的离散性预计会在细化极限下保持不变 [46]。

The Consistent Boundary Formalism

一致边界形式主义

Many discretized quantum systems, including spin foams, are formulated in terms of amplitudes that localize onto building blocks. The amplitude for a lattice built out of many building blocks is then given by the product over the amplitudes associated with each of the building blocks. Coarse graining such a lattice, i.e., integrating over some choice of finer data, leads generically to couplings between neighboring building blocks. Specifically, one can expect a coupling between two building blocks to appear, if one integrates over some (finer) boundary data that are shared by both building blocks. Iterated coarse graining steps lead then to couplings between building blocks that are farther and farther apart.

包括自旋泡沫在内的许多离散量子系统，都是以局域在构造块上的振幅来表述的。由多个构造块搭建而成的格点，其振幅等于各构造块对应振幅的乘积。对这类格点做粗粒化 (即积分掉某种选择的精细数据)，通常会导致相邻构造块之间出现耦合。具体来说，如果积分掉两个构造块共有的 (更精细的) 边界数据，就可以预期二者之间会产生耦合。重复进行粗粒化步骤后，耦合会出现在相隔越来越远的构造块之间。

Such nonlocal amplitudes are difficult to deal with. They would require a profound change of frameworks used in (loop) quantum gravity, e.g., the generalized boundary formalism [47, 48] or the canonical formalism. Note that a canonical formalism can also be defined for discrete systems and in particular triangulations [38], but this requires (One can also define a canonical formalism for discrete systems on a regular lattice with nonlocal actions. But a framework for systems on non-regular lattices with nonlocal actions has, to the best knowledge of the authors, not been developed yet.) an action localized onto building blocks.

这类非局域振幅难以处理，它们要求圈量子引力中使用的框架 (例如广义边界形式主义 [47,48] 或正则形式主义) 发生深刻变革。注意，正则形式主义也可以定义在离散系统特别是三角剖分上 [38]，但这要求作用量局域在构造块上 (也可以给具有非局域作用量的规则格点上的离散系统定义正则形式主义，但据作者所知，目前尚未开发出适用于具有非局域作用量的非规则格点系统的框架)。

We will now introduce the consistent boundary formalism [49,50], which allows to keep the locality of amplitudes. Here we trade nonlocal couplings for building blocks with more and more boundary data. Indeed, gluing building blocks (in $d \geq 2$ spacetime dimensions), each with a given amount of boundary data, we usually obtain a block that has more boundary data; see Fig. 1. Instead of referring to the glued blocks as being larger (In gravity the size of the building block would be rather part of the variables.), we say that these come with finer boundary data.

我们现在将介绍一致边界形式主义 [49,50]，它可以保持振幅的局域性。在这里，我们用拥有越来越多边界数据的构造块替换了非局域耦合。实际上，将 ($d \geq 2$ 时空维中的) 各带有限边界数据的构造块粘合后，我们通常会得到一个拥有更多边界数据的块；参见图 1。我们不将粘合后的块称为更大的块 (在引力中，构造块的大小更应当是变量的一部分)，而是认为它们带有更精细的边界数据。

Even if one is able to construct the amplitudes for arbitrarily fine boundary data, one often rather wishes to compute with a certain coarse set of data. Here we wish again for a notion of ”perfect” amplitudes, i.e., amplitudes which mirror exactly those obtained in an infinite refinement limit for the boundary data. Such a notion is given by cylindrically consistent amplitudes.

即使人们能够构造出任意精细边界数据对应的振幅，通常也更希望针对某组粗化数据进行计算。在这里我们同样需要一个“完美”振幅的概念，即能够精确复刻无限精修极限下边界数据所得振幅的振幅。柱一致振幅就提供了这样一个概念。

To explain this notion, we will review some formalism. We associate a boundary Hilbert space $\mathcal{H}_b$ to a given building block. The label b will indicate the fineness of the boundary (data). We will assume a directed partial ordering $\prec$ on the set of labels: $b \prec b'$ means that b' carries a finer set of boundary data than b . We will then assume that for each pair $b \prec b'$, there exists an embedding map $\iota_{b'b} : \mathcal{H}_b \to \mathcal{H}_{b'}$. These maps have to satisfy $\iota_{b''b'} \circ \iota_{b'b} = \iota_{b''b}$, for any triple $b'' \succ b' \succ b$.

为了解释这个概念，我们会回顾一些形式体系。我们给每个构造块关联一个边界希尔伯特空间 $\mathcal{H}_b$ 。标签 b 用于标识边界 (数据) 的精细程度。我们假设标签集合上存在一个有向偏序 $\prec : b \prec b'$ 表示 b' 携带的边界数据集比 b 更精细。接下来我们假设，对每个对 $b \prec b'$ ，都存在一个嵌入映射 $\iota_{b'b} : \mathcal{H}_b \to \mathcal{H}_{b'}$ 。对任意三元组 $b'' \succ b' \succ b$ ，这些映射必须满足 $\iota_{b''b'} \circ \iota_{b'b} = \iota_{b''b}$ 。

These maps relate coarser to finer Hilbert spaces and thus allow to interpret coarse data in terms of finer data. Given a directed partial ordered set of labels $\{b\}$, associated Hilbert spaces, and consistent embedding maps, a continuum Hilbert space $\mathcal{H}$ can be defined as inductive (or direct) limit:

这些映射关联了更粗和更细的希尔伯特空间，因此允许我们用更细数据来解释粗数据。给定一个标签的有向偏序集 $\{b\}$ 、关联的希尔伯特空间，以及一致嵌入映射，连续希尔伯特空间 $\mathcal{H}$ 可以定义为归纳 (或直接) 极限:

$$\mathcal{H} = \overline{\cup_b \mathcal{H}_b / \sim}. \tag{13}$$

That is, one takes the disjoint union of all Hilbert space $\mathcal{H}_b$, but mods out by an equivalence relation. Two states are equivalent, if they can be refined to the same state. To obtain a Hilbert space, one takes a completion of this union. To this end, one demands that the inner products for the Hilbert spaces $\mathcal{H}_b$ are also cylindrically consistent, that is, satisfy $\langle \psi_b \mid \chi_b \rangle_b = \langle \iota_{b'b}(\psi_b) \mid \iota_{b'b}(\chi_b) \rangle_{b'}$ for any pair $b' \succ b$.

也就是说，我们取所有希尔伯特空间 $\mathcal{H}_b$ 的不交并，再模掉一个等价关系。若两个态可以加细为同一个态，则它们等价。为得到希尔伯特空间，我们对该并取完备化。为此，要求希尔伯特空间 $\mathcal{H}_b$ 的内积也满足柱一致条件，即对任意一对 $b' \succ b$ 满足 $\langle \psi_b \mid \chi_b \rangle_b = \langle \iota_{b'b}(\psi_b) \mid \iota_{b'b}(\chi_b) \rangle_{b'}$ 。

Canonical loop quantum gravity is based on such constructions of kinematical continuum Hilbert spaces [51-56]. Here we emphasize "kinematical," as the embedding maps implement a notion of localizable kinematical vacuum states, which can be also understood as being derived from amplitudes of topological quantum field theories [56]. The Ashtekar-Lewandowski [51,52] vacuum is peaked on sharply vanishing electric fluxes, whereas the BF -vacuum [54-56] is based on sharply vanishing curvature. The embedding maps act by putting all finer degrees of freedom into the corresponding vacuum state. We will see below that it would be ideal to have rather embedding maps, which put the finer degrees of freedom into a physical vacuum state, that is, a vacuum state defined by the dynamics of the system.

正则圈量子引力建立在这类运动学连续希尔伯特空间的构造之上 [51-56]。此处我们强调“运动学”，因为嵌入映射实现了可局域化运动学真空态的概念，这也可以理解为源自拓扑量子场论的振幅 [56]。阿西卡-莱万多夫斯基真空 [51,52] 峰值在电通量严格为零处，而 BF 真空 [54-56] 建立在曲率严格为零的基础上。嵌入映射通过将所有更细的自由度置于相应真空态来作用。我们下文会看到，理想的情况是拥有能将更细自由度置于物理真空态 (即由系统动力学定义的真空态) 的嵌入映射。

Operators $\mathcal{O}$ on $\mathcal{H}$ can be defined as families of operators $\{\mathcal{O}_b\}_b$, which are cylindrically consistent, that is, satisfy $\iota_{b'b}\mathcal{O}_b(\psi_b) = \mathcal{O}_{b'}(\iota_{b'b}(\psi_b))$ for all $b' \succ b$. The different vacua and associated embedding maps do also implement different notions of coarse graining for the operators and corresponding classical phase space functions [57, 58] .

$\mathcal{H}$ 上的算符 $\mathcal{O}$ 可以定义为满足柱一致性的算符族 $\{\mathcal{O}_b\}_b$ ，即对所有 $b' \succ b$ 满足 $\iota_{b'b}\mathcal{O}_b(\psi_b) = \mathcal{O}_{b'}(\iota_{b'b}(\psi_b))$ 。不同的真空和对应的嵌入映射也给算符和相应经典相空间函数 [57, 58] 实现了不同的粗粒化概念。

Let us assume that we have a directed and partially ordered set of boundary Hilbert spaces $\{\mathcal{H}_b\}_b$, with consistent embedding maps. A cylindrically consistent set of amplitudes $\{\mathcal{A}_b\}_b$ is then defined to be a set of linear functionals on $\mathcal{H}_b$, satisfying $\mathcal{A}_b(\psi_b) = \mathcal{A}_{b'}(\iota_{b'b}(\psi_b))$ for every pair $b' \succ b$, or equivalently

假设我们有一个带方向的偏序边界希尔伯特空间集 $\{\mathcal{H}_b\}_b$ ，且存在一致嵌入映射。柱一致振幅集 $\{\mathcal{A}_b\}_b$ 被定义为 $\mathcal{H}_b$ 上的线性泛函集，对每一对 $b' \succ b$ 满足 $\mathcal{A}_b(\psi_b) = \mathcal{A}_{b'}(\iota_{b'b}(\psi_b))$ ，等价于

$$\mathcal{A}_b = \iota^*_{b'b}\mathcal{A}_{b'}, \tag{14}$$

where $\iota^*_{b'b}$ denotes the pullback of $\psi_{b'b}$.

其中 $\iota^*_{b'b}$ 表示 $\psi_{b'b}$ 的拉回。

The cylindrically consistent amplitudes allow us to define continuum amplitudes on the continuum Hilbert space (13). It also makes precise the notion of mirroring the continuum dynamics: the embedding maps allow to interpret discrete states ψ_b as continuum states, and the cylindrically consistent amplitudes make sure that one obtains the same results for different refinements of a given boundary state ψ_b .

柱一致振幅允许我们在连续希尔伯特空间 (13) 上定义连续振幅。它也明确了连续动力学镜像的概念: 嵌入映射允许我们将离散态 ψ_b 解释为连续态，而柱一致振幅保证了对给定边界态 ψ_b 的不同加细都能得到相同的结果。

How to construct such cylindrically consistent amplitudes? This can again be done in an iterative procedure. Starting with amplitudes $\mathcal{A}_b$ for building blocks with boundary b , we glue these to a block with finer boundary b' ; see Fig. 2. The gluing operation includes to integrate the product of amplitudes over the data that are bulk in the new block. In this way we obtain an amplitude $\mathcal{A}_{b'}$ for a finer boundary.

如何构造满足柱一致性的振幅？这同样可以通过迭代过程实现。从带有边界 b 的构建块的振幅 $\mathcal{A}_b$ 出发，我们将其粘合到带有更细边界 b' 的块上；参见图 2。粘合操作包括对新块中属于体区域的数据积分振幅乘积，通过这种方式我们得到更细边界对应的振幅 $\mathcal{A}_{b'}$ 。

To improve the discrete amplitudes in an iterative scheme, similar to the ones discussed in section "The Need for Renormalization: Restoring Diffeomorphism Symmetry," we need a fixed point condition. To this end we need to construct out of $\mathcal{A}_{b'}$ an amplitude for a building block with boundary b . Thus we use an embedding map to define an improved amplitude $\mathcal{A}'_b$:

若要在迭代方案中改进离散振幅，类似于“重整化的必要性: 恢复微分同胚对称性”一节讨论的方案，我们需要一个不动点条件。为此我们需要从 $\mathcal{A}_{b'}$ 出发，构造带有边界 b 的构建块的振幅。因此我们使用嵌入映射来定义改进后的振幅 $\mathcal{A}'_b$:

$$\mathcal{A}'_b = \iota^*_{b'b}\left(\sum_{\text{bulk}}\prod_i \mathcal{A}_{i,b}\right). \tag{15}$$

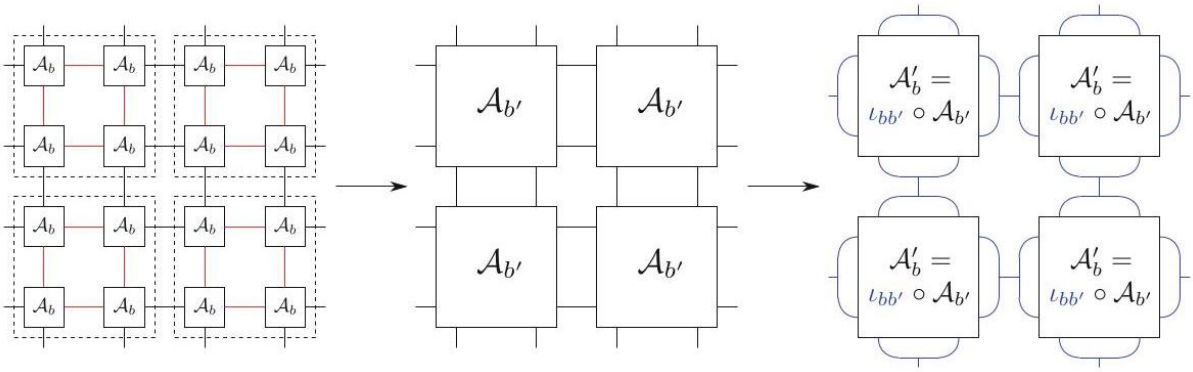

Fig. 2 Schematics for coarse graining spin foam amplitude: among the degrees of freedom, some (here in red) are defined as fine and summed over. The remaining effective amplitude has a refined boundary b'. Embedding maps $\iota_{bb'}$ in blue map to the original Hilbert space of the coarse boundary b, and we define the renormalized amplitude $\mathcal{A}'_b$

图 2 自旋泡沫振幅粗粒化示意图: 在自由度中，部分自由度 (此处为红色) 被定义为细自由度并被求和。剩余有效振幅具有细化边界 b'。蓝色的嵌入映射 $\iota_{bb'}$ 映射到粗边界 b 的原始希尔伯特空间，我们由此定义重整化振幅 $\mathcal{A}'_b$

This process can be iterated, until a fixed point is reached, that is,

这个过程可以迭代，直到达到不动点，即

$$\mathcal{A}^{\text{fix}}_b = \iota^*_{b'b}\left(\sum_{\text{bulk}}\prod_i \mathcal{A}^{\text{fix}}_{i,b}\right). \tag{16}$$

If $\mathcal{A}^{\text{fix}}_b$ does not depend on the choice of the finer boundary b' in this construction, it can serve as the b-component of a cylindrically consistent family of amplitudes. Note that this is often not the case. But for fixed b and finer and finer b', one uses a finer and finer discretization to compute the amplitude for a coarse boundary b. Thus the series of amplitudes $\left\{\mathcal{A}^{\text{fix}}_b(b')\right\}_{b'}$ is expected to converge; see [49] for examples.

如果在该构造中 $\mathcal{A}^{\text{fix}}_b$ 不依赖于更细边界 b' 的选择，它就可以作为柱一致振幅族的 b 分量。请注意，情况通常并非如此。但对于固定的 b 和越来越细的 b'，我们使用越来越细的离散化来计算粗边界 b 的振幅。因此振幅序列 $\left\{\mathcal{A}^{\text{fix}}_b(b')\right\}_{b'}$ 有望收敛；例子参见文献 [49]。

The resulting fixed point amplitudes will depend on the choice of embedding maps $\iota_{b'b}$ and might lead to non-sensible results for certain choices [49]. For example, choosing the kinematical embedding maps described above will often result in amplitudes that just describe the associated vacuum states of topological field theories, even if the starting point is a theory with propagating degrees of freedom.

最终得到的不动点振幅依赖于嵌入映射 $\iota_{b'b}$ 的选择，某些选择可能会得到不合理的结果 [49]。例如，选择上文描述的运动学嵌入映射，通常得到的振幅只能描述拓扑场论的相关真空态，即使初始理论是带有传播自由度的理论。

To avoid this, it is important to determine the embedding maps from the dynamics of the system. This also means that the embedding maps might change throughout the coarse graining algorithms. Below, we will describe tensor network algorithms, which do implement embedding maps, adapted to the dynamics.

为了避免这种情况，从系统动力学出发确定嵌入映射十分重要。这也意味着嵌入映射可能在粗粒化算法过程中发生变化。下文我们将描述实现了适配动力学的嵌入映射的张量网络算法。

The need for choosing embedding maps, which are informed by the dynamics, is even more important for systems with diffeomorphism symmetry. In fact, the ideal embedding maps are given by amplitudes describing the evolution of a coarser into a finer boundary. To explain this, we remind the reader that for systems with diffeomorphism symmetry, the path integral does not implement a proper time evolution, but is rather a projector onto the space of gauge invariant, so-called physical, states.

对于具有微分同胚对称性的系统，选择符合动力学要求的嵌入映射更为重要。实际上，理想的嵌入映射由描述从较粗边界到较细边界演化的振幅给出。为了解释这一点，我们提醒读者，对于具有微分同胚对称性的系统，路径积分并不实现正常时间演化，而是一个投影到规范不变的所谓物理态空间上的投影器。

Assume we can embed states associated with discrete boundaries $b \prec b'$ into a continuum Hilbert space and compute the continuum path integral "propagating" the embedded states defined from b to states defined from the finer b' . The resulting amplitude $\mathcal{A}_{b'b}$ then (i) projects out any gauge dependence from the b -states and (ii) associates to all the finer degrees of freedom a physical vacuum state [59].

假设我们可以将离散边界 $b \prec b'$ 对应的态嵌入连续希尔伯特空间，并计算从 b 定义的嵌入态“传播”到更细 b' 定义的态的连续路径积分。由此得到的振幅 $\mathcal{A}_{b'b}$ 会:(i) 从 b 态中投影掉所有规范依赖，(ii) 为所有更细自由度关联一个物理真空态 [59]。

An ideal choice for the embedding maps is then given by these refining amplitudes $\iota_{b'b} = \mathcal{A}_{b'b}$. With this choice, we satisfy the cylindrical consistency condition (14) for the amplitudes $\mathcal{A}_b \equiv \mathcal{A}_{b\varnothing}$ [50]. Here $\mathcal{A}_{b\varnothing}$ is constructed as described above, with $\varnothing$ denoting the "empty" boundary. That is, we compute the continuum path integral for a block with boundary b .

对于嵌入映射，这些细化振幅 $\iota_{b'b} = \mathcal{A}_{b'b}$ 是理想的选择。采用该选择，我们就能满足振幅 $\mathcal{A}_b \equiv \mathcal{A}_{b\varnothing}$ 的柱一致性条件 (14) [50]。此处 $\mathcal{A}_{b\varnothing}$ 按上述方法构造，其中 $\varnothing$ 表示“空”边界。也就是说，我们对带有边界 b 的区块计算连续路径积分。

The consistency condition can now be expressed as

一致性条件现在可以表述为

$$\mathcal{A}_{b\varnothing} = \mathcal{A}_{bb'} \circ \mathcal{A}_{b'\varnothing}, \tag{17}$$

where $\circ$ includes integrating or summing over the data associated with the boundary b'. This has to hold for any $b' \succ b$. We assumed that the amplitudes result from a continuum path integral; they should therefore be discretization independent. Equation (17) does express such a notion of discretization independence, namely, that the final amplitude should not depend on the number of building blocks or evolution steps.

其中 $\circ$ 包含对与边界 b' 相关联的数据进行积分或求和，这对任意 $b' \succ b$ 都必须成立。我们假定振幅由连续路径积分得到，因此它们应当与离散化无关。方程 (17) 恰好表达了这种离散化无关性的概念，即最终振幅不应依赖于构造块的数量或演化步数。

We thus see that for diffeomorphism invariant systems, the embedding maps should be given by the amplitudes. In this way the embedding maps do also describe the physical vacuum state for the given system. These concepts can be realized for topological quantum field theories [56, 59] .

因此我们可以看到，对于微分同胚不变系统，嵌入映射应由振幅给出。通过这种方式，嵌入映射也可以描述给定系统的物理真空态。这些概念可以在拓扑量子场论 [56, 59] 中实现。

The situation is much more involved for interacting systems. Often, one can only resort to numerical schemes. We will discuss next tensor network algorithms, which implement a coarse graining flow (15), with a dynamically determined embedding map. In fact, embedding maps are constructed using a localized form of the transfer operator method, which also serves to identify vacuum states.

对于相互作用系统，情况要复杂得多。通常来说，人们只能借助数值方法。接下来我们将讨论张量网络算法，这类算法实现了粗粒化流 (15)，并带有动态确定的嵌入映射。实际上，嵌入映射是通过转移算子方法的局域形式构造的，该方法也可用于识别真空态。

Tensor Network Renormalization

张量网络重整化

A concrete numerical realization of the consistent boundary formulation for physical systems are tensor network methods. Here we mostly discuss the ”tensor network renormalization group” (TNRG) [60] as variations of it were used in all spin foam-related research. TNRG can also be understood as a generalization of corner transfer matrix methods for 2D systems [61].

张量网络方法是物理系统一致边界表述的具体数值实现。本文我们主要讨论“张量网络重整化群”(TNRG)[60]，因为所有与自旋泡沫相关的研究都使用了它的变体。TNRG 也可被理解为二维系统角转移矩阵方法的推广 [61]。

The key idea of TNRG is to cast the partition function of a physical system into a tensor network, a contraction of tensors, and then to manipulate this network to approximate it by a coarser network of effective tensors. This defines a renormalization flow of tensors while keeping the description of the system local: tensors only interact with their direct neighbors. Here, a tensor is a multidimensional array associated with a region of the physical system. Its labels correspond to (a basis of) the boundary data of that region, and for each choice of boundary data, it stores the associated amplitude. In this sense, a tensor is similar to spin foam amplitudes as it associates an amplitude to a region as a function of its boundary data [62,63]. We represent

such a tensor pictorially by a node with several legs, one leg for each index of the tensor. Note that these tensors do not make a reference to a background spacetime; they merely encode the degrees of freedom of the system. In this regard they are well suited to be applied to quantum gravity.

TNRG 的核心思想是将物理系统的配分函数改写为张量网络 (即张量的缩并)，随后对该网络进行操作，用有效张量构成的更粗网络对其做近似。这一定义了张量的重整化流，同时保持了对系统的局域描述: 张量仅与其直接相邻的张量相互作用。此处，张量是与物理系统的一个区域关联的多维数组。它的指标对应于该区域边界数据 (的一组基)，对于每一组边界数据，张量存储了对应的振幅。从这个意义上说，张量类似自旋泡沫振幅，它作为边界数据的函数，将振幅关联到一个区域 [62,63]。我们用带多个支腿的节点对张量做图示表示，每一个支腿对应张量的一个指标。注意这些张量不依赖背景时空；它们仅编码系统的自由度。就此而言，它们非常适合应用于量子引力。

Having identified a tensor as the amplitude associated with a region, the next step is to glue tensors together. To do so we identify the shared boundary data of two tensors and sum over all possible values these shared data can take, i.e., we contract their indices. Pictorially we represent this contraction by connecting the respective legs of the nodes. Continuing this process, we build a network of tensors, whose contraction defines the partition function.

在明确张量是关联到区域的振幅后，下一步就是将张量粘合在一起。具体操作是匹配两个张量共享的边界数据，对这些共享数据所有可能的取值求和，也就是对它们的指标做缩并。图示上我们通过连接节点对应的支腿表示缩并。不断重复这个过程，我们就构建出一个张量网络，该网络的缩并就定义了配分函数。

The goal of a coarse graining step is to approximate the original tensor network by a coarse tensor network. The coarse tensor network is then the starting point for the next iteration of the algorithm. There exist many realizations of the TNRG, and they all have two steps in common: explicit summation over fine (bulk) degrees of freedom as well as variable transformations and truncations of (boundary) degrees of freedom to define effective boundary Hilbert spaces. These variable transformations play the role of (inverse) embedding maps mentioned above, as they directly translate fine into coarse degrees of freedom. Crucially, the embedding maps are computed from the tensors in each iteration of the algorithm via a singular value decomposition. Thus, the embedding maps can change in each iteration and are in fact chosen according to the dynamics encoded by the tensors.

粗粒化步骤的目标是用粗张量网络近似原张量网络，得到的粗张量网络会作为算法下一次迭代的起点。目前存在多种 TNRG 实现，它们都共有两个步骤: 对细 (体) 自由度做显式求和，以及对 (边界) 自由度做变量变换与截断，以定义有效边界希尔伯特空间。这些变量变换起到上文提到的 (逆) 嵌入映射的作用，直接将细自由度转化为粗自由度。关键在于，嵌入映射是在算法每次迭代中通过奇异值分解从张量计算得到的。因此，嵌入映射在每次迭代中都可以改变，并且实际上是根据张量编码的动力学来选择的。

Without going into the details of the algorithms, we will briefly explain the role of the singular value decomposition (SVD) in defining the embedding maps. A SVD decomposes a matrix M into two unitary matrices U and V and a diagonal matrix $\lambda, M = U\lambda V^\dagger$. It is applicable to real and complex matrices, where M need not be a rectangular matrix. The matrices U and V are matrices of left and right singular vectors, respectively, the entries λ_i of the diagonal matrix λ are called singular values. Crucially, the singular values are real, non-negative and ordered in size, $\lambda_1 \geq \lambda_2 \geq \cdots \geq \lambda_N \geq 0$. Hence, the size of the singular values

relative to the largest one determines how relevant the associated singular vectors of U and V are to reconstruct M . On the other hand, we can define the optimal approximation (in the least square sense) of M by a matrix of rank $D < N$ by setting all singular values $i > D$ to zero [60, 64] . So, if the singular values decreases rapidly relative to the largest one, it is possible to approximate the matrix M by a matrix of lower rank.

我们不讨论算法细节，仅简要解释奇异值分解 (SVD) 在定义嵌入映射中的作用。SVD 将矩阵 M 分解为两个幺正矩阵 U 、V 和一个对角矩阵 $\lambda, M = U\lambda V^{\dagger}$ 。它适用于实矩阵和复矩阵，其中 M 不必是矩形矩阵。矩阵 U 和 V 分别是左奇异向量矩阵和右奇异向量矩阵，对角矩阵 λ 的元素 λ_i 称为奇异值。关键在于，奇异值均为非负实数，且按大小排序 $\lambda_1 \geq \lambda_2 \geq \cdots \geq \lambda_N \geq 0$ 。因此，相对于最大奇异值，奇异值的大小决定了对应奇异向量在 U 和 V 重构 M 中的重要程度。另一方面，我们可以通过将所有奇异值 $i > D$ 置零 [60, 64] ，得到秩为 $D < N$ 的矩阵对 M 的最优近似 (最小二乘意义下)。因此，如果奇异值相对于最大奇异值衰减很快，就可以用低秩矩阵近似矩阵 M 。

How can this matrix decomposition be used to coarse grain tensors? Ideally we would like to directly split tensors into multiple tensors of lower rank. We can then recombine those into new effective tensors by contracting the original indices. Unfortunately, a decomposition analogous to SVDs does not exist for tensors. Instead, we rearrange the tensor into a matrix, by grouping its indices into two matrix indices. These matrix indices simply label the product basis of the boundary Hilbert spaces of the grouped tensor labels. Now, we decompose this matrix using a SVD: the matrices U and V define the variable transformations of the old product basis into a new effective one labeled and ordered by the singular values. We show an example of such a decomposition in Fig. 3. From the relative size of these singular values follows the relative relevance of the corresponding singular vectors for reconstructing the tensor. With this information, we truncate the most irrelevant singular values/vectors, e.g., by always truncating after a fixed number of singular values or only considering singular values above a certain size relative to the largest one. Once we have obtained the singular vectors, we translate the product basis back into the original tensor indices and thus define a split tensor.

这种矩阵分解如何用于张量粗粒化？理想情况下我们希望直接将张量拆分为多个低秩张量，再通过缩并原指标将它们重新组合为新的有效张量。遗憾的是，张量不存在类似 SVD 的分解方法。我们转而将张量整理为矩阵: 把它的指标分组为两个矩阵指标，这些矩阵指标仅用来标记分组后张量边界希尔伯特空间乘积基的标签。现在我们用 SVD 分解这个矩阵: 得到的矩阵 U 和 V 定义了从旧乘积基到按奇异值标记排序的新有效基的变量变换。我们在图 3 中给出了这种分解的示例。根据这些奇异值的相对大小，可以得到对应奇异向量对重构张量的相对重要程度。利用这一信息，我们截断最不重要的奇异值/向量，例如可以固定保留奇异值的数量，截断剩余部分；或者仅保留相对最大奇异值高于某一阈值的奇异值。得到奇异向量后，我们将乘积基转换回原张量指标，从而得到拆分后的张量。

Figures 3 and 4 illustrate one coarse graining step. First, we sum over fine degrees of freedom resulting in a new tensor with more boundary data. We rearrange its indices with the goal to split into two tensors, a 3-valent one containing the two upward-pointing indices and a 7-valent one with the remaining indices. The new edge of the tensors will be labeled by the singular values obtained in the decomposition. The 3-valent tensor defines a unitary embedding map. Without truncations they act as isometries between different basis of the boundary Hilbert spaces.

图 3 和图 4 展示了一次粗粒化步骤。首先我们对细粒度自由度求和，得到一个拥有更多边界数据的新张量。我们整理它的指标，目标是将其拆分为两个张量: 一个 3 价张量包含两个向上指标，一个 7 价张量包含剩余指标。张量的新边将由分解得到的奇异值标记。3 价张量定义了一个酉嵌入映射，不做截断时它们是边界希尔伯特空间不同基之间的等距映射。

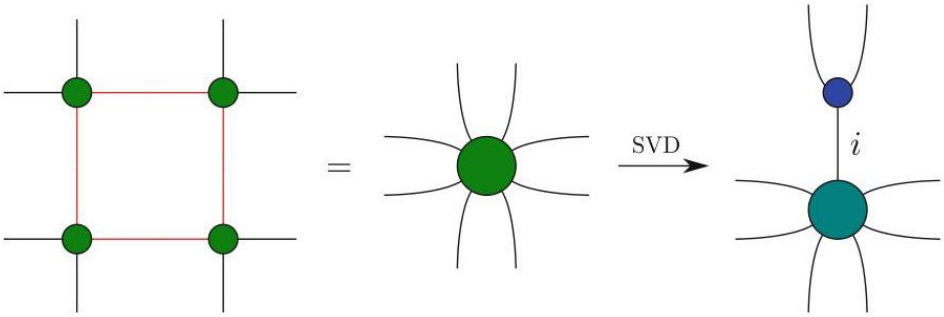

Fig. 3 After the contraction of fine indices (red), we obtain a new tensor with eight legs. To decompose it, we turn it into a matrix by grouping its indices into two groups: the upward-pointing indices form one group, with all remaining indices in the other. After the SVD, we obtain two tensors, a 3-valent and a 7-valent one. We use the 3-valent one as an embedding map, as it translates fine into coarse degrees of freedom

Fig. 3 缩并细指标 (红色) 后，我们得到一个拥有八条腿的新张量。为了分解它，我们将其指标分为两组，整理为矩阵: 向上指标为一组，其余所有指标为另一组。SVD 分解后我们得到两个张量，一个 3 价，一个 7 价。我们将 3 价张量用作嵌入映射，因为它实现了细粒度自由度到粗粒度自由度的转换。

Fig. 4 After the contraction and computation of embedding maps via a SVD, we contract all fine boundary legs of the effective tensor with embedding maps. They translate fine into coarse degrees of freedom and introduce truncations. A coarse network of renormalized tensors remains

Fig. 4 完成缩并并通过 SVD 计算得到嵌入映射后，我们将有效张量的所有细边界腿与嵌入映射缩并。它们完成了细粒度自由度到粗粒度自由度的转换，同时引入截断，最终得到由重整化张量构成的粗粒化网络。

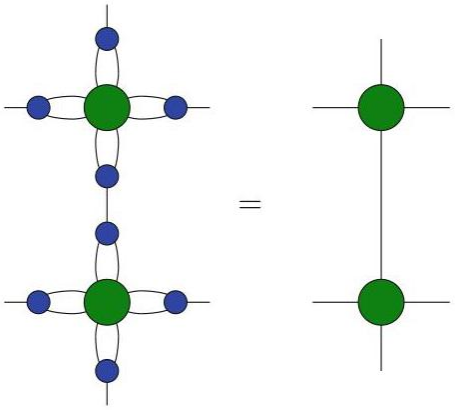

However, truncations are necessary, since the coarse boundary Hilbert spaces grow exponentially with each iteration. Keeping track of the size of the truncated singular values (relative to the largest ones) makes it possible to characterize the truncation error. In the final step, the fine boundary data of the tensors get contracted with the 3-valent embedding maps, resulting in a renormalized tensor with coarse boundary data.

然而，截断是必要的，因为粗边界希尔伯特空间的规模会随每次迭代指数增长。记录截断后奇异值相对最大奇异值的大小，可以刻画截断误差。在最后一步，张量的细边界数据会与 3 价嵌入映射缩并，得到带有粗边界数据的重整化张量。

Tensor Networks and Spin Foams

张量网络与自旋泡沫

In many ways, TNRG is well suited for spin foams. The method does not require a background spacetime; the concept of tensors and their boundary data is similar to spin foam amplitudes and the method, in contrast to Monte Carlo sampling, works well for complex and oscillating amplitudes: in TNRG we explicitly sum over fine degrees of freedom instead of sampling over them. However, spin foams cannot be readily cast into tensor network form for two reasons: firstly, tensor networks are built under the assumption that degrees of freedom are only shared between two tensors. For spin foams this condition is not fulfilled: here, tetrahedra and triangles are decorated by algebraic data. While a tetrahedron is only shared among two 4- simplices, a triangle can belong to several 4-simplices. Assigning a tensor to each 4-simplex, only a part of the spin foam state-sum can be expressed as a contraction of a tensor network. This insight is useful for optimizing numerical algorithms [65], yet it is not sufficient for coarse graining à la TNRG. As we will argue below, spin foams require a generalization of this formalism called decorated tensor networks.

在很多方面，TNRG 都非常适合自旋泡沫模型。该方法不需要背景时空；张量及其边界数据的概念与自旋泡沫振幅相似，而且和蒙特卡洛采样不同，该方法对复杂振荡振幅效果良好: 在 TNRG 中，我们会对精细自由度显式求和，而非对其采样。但自旋泡沫无法直接转化为张量网络形式，原因有二: 首先，张量网络构建的前提是自由度仅由两个张量共享。自旋泡沫并不满足这一条件: 在自旋泡沫中，四面体和三角形由代数数据标记。四面体仅由两个四维单形共享，但一个三角形可以属于多个四维单形。如果给每个四维单形分配一个张量，那么只有部分自旋泡沫状态和可以表示为张量网络缩并。这一结论对优化数值算法 [65] 很有用，但不足以实现 TNRG 风格的粗粒化。我们在下文中会说明，自旋泡沫需要对该形式体系进行推广，得到的就是装饰张量网络。

The second obstacle is that TNRG methods require finite tensors, e.g., with finite index ranges. In spin foams the representation labels on faces are typically unbounded. Introducing a cut-off on representation labels breaks gauge symmetry. A physically relevant exception are spin foams with non-vanishing cosmological constant, where the gauge-invariant cut-off is inversely proportional to the square-root of the cosmological constant. In recent years, several different spin foam models have been proposed [66-70]. One well-known 3D spin foam model with cosmological constant is the Turaev-Viro model [71], which uses a quantum deformation of SU(2) [72]. Such quantum deformations are also used in TNRG applications to (analogue) spin foam models [73-75].

第二个障碍是 TNRG 方法要求张量为有限张量，例如具有有限指标范围。而在自旋泡沫中，面上的表示标记通常是无界的。对表示标记引入截断会破坏规范对称性。一个符合物理规律的例外是带有非零宇宙学常数的自旋泡沫，这类模型中规范不变截断与宇宙学常数的平方根成反比。近年来，研究者已经提出了多种不同的自旋泡沫模型 [66-70]。一个著名的带宇宙学常数的三维自旋泡沫模型是图拉耶夫-维罗 (Turaev-Viro) 模型 [71]，该模型使用 SU(2) 的量子变形 [72]。这类量子变形也被应用于针对 (类比) 自旋泡沫模型的 TNRG 研究中 [73-75]。

Models with Global Symmetry: Spin Net Models

整体对称性模型: 自旋网模型

TNRG methods are primarily aimed at condensed matter systems with a global symmetry, the 2D Ising model being a prime example [60, 76]. Without external magnetic field, it possesses a global $\mathbb{Z}_2$ symmetry. Thanks to this property, it is straightforward to cast this model into tensor network language. One way to do so is to expand the system in terms of irreducible representations of its symmetry group, analogous to the familiar harmonic analysis of SU(2) used in LQG and spin foams. The boundary Hilbert spaces are tensor products of representation spaces of the underlying group where the tensor encodes the coupling rules. This construction (and the differences and similarities to spin foams) was first presented in [77] for finite groups before it was extended to quantum groups in [73, 74] . Such models with global symmetries are called spin net models.

TNRG 方法主要针对具有整体对称性的凝聚态系统，二维伊辛模型就是一个典型例子 [60, 76]。在无外磁场的情况下，它具有整体 $\mathbb{Z}_2$ 对称性。得益于这一性质，我们可以直接将该模型转化为张量网络语言。实现这一点的一种方法是用其对称群的不可约表示展开系统，这类似于圈量子引力 (LQG) 和自旋泡沫中常用的 SU(2) 调和分析。边界希尔伯特空间是基础群表示空间的张量积，张量在此编码耦合规则。这种构造 (以及它与自旋泡沫的异同) 最早于 [77] 中针对有限群提出，之后在 [73, 74] 中被推广到量子群。这类具有整体对称性的模型被称为自旋网模型。

TNRG methods were applied to 2D spin net models for various symmetry groups, namely, finite Abelian groups $\mathbb{Z}_q$ [62], the finite non-Abelian permutation group S_3 [78], and the quantum group $\mathrm{SU}(2)_k$ [73]. Models with $\mathrm{SU}(2)_k \times \mathrm{SU}(2)_k$ symmetry [75] mimic the construction of Euclidean 4D spin foam models, such as the Barrett-Crane [79] and the EPRL model [80]. Representation theory is used to optimize the algorithm and improve the interpretation of the coarse graining flow. For more detailed explanations, we refer the interested reader to the respective papers [62, 73, 75, 78] or this recent review [81].

TNRG 方法已被应用于不同对称群的二维自旋网模型，即有限阿贝尔群 $\mathbb{Z}_q$ [62]、有限非阿贝尔置换群 S_3 [78] 和量子群 $\mathrm{SU}(2)_k$ [73]。具有 $\mathrm{SU}(2)_k \times \mathrm{SU}(2)_k$ 对称性的模型 [75] 模仿了欧几里得四维自旋泡沫模型的构造，例如 Barrett-Crane 模型 [79] 和 EPRL 模型 [80]。该方法利用表示论优化算法，并提升了粗粒化流的可解释性。如需了解更多细节，感兴趣的读者可查阅相关论文 [62, 73, 75, 78] 或这篇近期综述 [81]。

The TNRG method is ideal to identify different phases of the model and map out its phase diagram. Here we define a phase as the region in parameter space for which the system flows to the same attractive fixed point under renormalization. Note that such attractive fixed points describe topological theories.

TNRG 方法非常适用于识别模型的不同相并绘制其相图。在此我们将相定义为参数空间中，系统重整化后流向同一吸引不动点的区域。请注意，这类吸引不动点描述的是拓扑理论。

In case the theory possesses multiple phases, we find phase transitions, which can feature interesting dynamics. Using TNRG methods, we gain insights into whether a phase transition is of first or higher order. For a first-order transition, the system quickly converges to either of the final fixed points, no matter how close we tune the parameters to the transition. The behavior is starkly different for transitions of higher order: close to the phase transition, the system remains almost the same for a number of iterations before it converges to either of the attractive fixed points. This indicates the presence of a repulsive fixed point and an approximate scale invariance. Close to such a transition, the singular values only slowly decrease in size, and truncations cannot be justified as the largest truncated singular value is close to the smallest kept one. This shows that more and more degrees of freedom are relevant, which hints at a diverging correlation length. In tensor network language, where we describe the system by locally interacting amplitudes, this translates to infinitely large boundary Hilbert spaces.

如果理论存在多个相，我们就会得到相变，相变可以呈现出有趣的动力学特性。利用 TNRG 方法，我们可以判断相变是一级还是更高阶。对于一级相变，无论我们将参数调整得多接近相变点，系统都会快速收敛到两个终态不动点中的一个。这种行为在高阶相变中截然不同: 在相变点附近，系统会在多轮迭代中几乎保持不变，之后才收敛到其中一个吸引不动点。这表明存在一个排斥不动点和近似标度不变性。在这类相变附近，奇异值的大小下降非常缓慢，截断不再合理，因为被截断的最大奇异值与保留的最小奇异值大小接近。这说明越来越多的自由度变得相关，暗示关联长度发散。在张量网络语言中 (我们用局域相互作用振幅描述系统)，这对应着无穷大的边界希尔伯特空间。

Before we discuss renormalizing gauge theories, let us briefly mention some disadvantages of TNRG that were addressed in later schemes like tensor network renormalization (TNR) [76]. In particular for higher accuracy, i.e., taking many singular values into account, TNRG converges to ”unphysical” fixed points. They are highly dependent on the initial conditions, which can obstruct identifying the correct renormalization group flow and universality classes. This issue is addressed by entanglement filtering: it identifies and removes short scale entanglement, which avoids the occurrence of these particular fixed points.

在讨论规范理论的重整化之前，我们简要说明 TNRG 的一些缺点，这些缺点在后续的张量网络重整化 (TNR) 等方案中得到了解决 [76]。若要求更高精度，即保留更多奇异值，TNRG 会收敛到“非物理”不动点。这类不动点高度依赖初始条件，会阻碍我们识别正确的重整化群流和普适类。纠缠过滤解决了这个问题: 它识别并去除短程纠缠，避免了这类特殊不动点的出现。

Local Symmetries: Decorated Tensor Networks and the Fusion Basis

定域对称性: 装饰张量网络与融合基

As mentioned above, for systems with local gauge symmetry, like spin foams, we cannot readily apply methods like TNRG. Gauge systems encode redundantly degrees of freedom into local variables, which are subject to Gauss constraints. This increases the computational costs for TNRG, as these scales exponentially with the number of variables per building block.

如上所述，对于自旋泡沫这类具有定域规范对称性的系统，我们无法直接应用 TNRG 这类方法。规范系统将自由度冗余编码到受高斯约束限制的定域变量中。这会增加 TNRG 的计算成本，因为计算量会随每个构造块的变量数量呈指数增长。

Instead of expressing lattice gauge theories strictly as tensor networks, [63] proposes to use decorated tensor networks. Here decorations refer to labels associated with lower dimensional boundary components. We consider the amplitudes associated with spacetime regions and their boundary states, e.g., 3D cubes equipped with spin network states, as the fundamental objects of the system which we intend to renormalize. Coarse graining is performed analogous to TNRG methods: these amplitudes are split by using a SVD and then rearranged into new effective ones, where we sum over bulk degrees of freedom. The key to this algorithm is the boundary Hilbert space: firstly, to implement this procedure economically, we solve for all Gauss constraints and explicitly express redundant variables as functions of the remaining ones. This corresponds to choosing a maximal tree in the spin network. Secondly, this maximal tree must be chosen with the intended splitting in mind: the remaining variables are distributed equally across the two split amplitudes and the data shared between them. Given this distinction, we define matrices that can be split by a SVD. Variables belonging to either split amplitude are summarized in either index of the matrix, while we keep the shared variables fixed. We then perform the decomposition for each shared configuration. This reduces numerical costs. Finally, the maximal tree is adapted again for the gluing of partial amplitudes into a final effective one. This algorithm is illustrated in Fig. 5. To lowest accuracy, we keep a single singular value per shared configuration of the original amplitude. In case we retain more singular values, each face of the renormalized building block carries an additional index. This gives the name to this algorithm as the tensor network is ”decorated” with an intricate boundary Hilbert space. This algorithm was successfully applied to 3 d$\mathbb{Z}_2$ lattice gauge theory and identified the phase transition between weak and strong coupling phase to reasonable accuracy [63].

文献 [63] 没有将格点规范理论直接表示为张量网络，而是提出使用装饰张量网络。此处的“装饰”指与低维边界分量关联的标签。我们将时空区域及其边界态关联的振幅 (例如配备自旋网络态的三维立方体) 作为我们要重整化的系统的基本对象。粗粒化的实现与 TNRG 方法类似: 利用奇异值分解拆分这些振幅，再将其重排为新的有效振幅，过程中对体自由度求和。该算法的核心在于边界希尔伯特空间: 首先，为了高效实现该流程，我们对所有高斯约束求解，将冗余变量显式表示为剩余变量的函数，这对应于在自旋网络中选择一棵极大树。其次，选择极大树时需要考虑预设的拆分方案: 将剩余变量均匀分配到两个拆分振幅和它们共享的数据中。基于这一区分，我们定义可通过奇异值分解拆分的矩阵，属于各拆分振幅的变量分别放在矩阵的两个指标中，同时固定共享变量，随后对每个共享构型做分解，这降低了数值计算成本。最后，再次调整极大树，将分振幅粘合为最终的有效振幅。该算法如图 5 所示。最低精度设置下，原振幅的每个共享构型保留一个奇异值。如果保留更多奇异值，重整化构造块的每个面会携带一个额外指标。这就是该算法名称的由来——张量网络被复杂的边界希尔伯特空间“装饰”。该算法已成功应用于 3 d$\mathbb{Z}_2$ 格点规范理论，并在合理精度下识别出弱耦合相与强耦合相之间的相变 [63]。

Fig. 5 Graphical illustration of the decorated tensor network algorithm for Abelian gauge theories: the boundary Hilbert space is spanned by spin network states. The bold edges show the non-gauge fixed variables. The cubes are split by a singular value decomposition in two different ways. The resulting prism amplitudes are recombined into a coarse-grained cube

图 5 阿贝尔规范理论装饰张量网络算法的图示说明: 边界希尔伯特空间由自旋网络态张成，粗边表示未做规范固定的变量。立方体通过奇异值分解以两种不同方式拆分，得到的棱柱振幅重新组合为一个粗粒化立方体

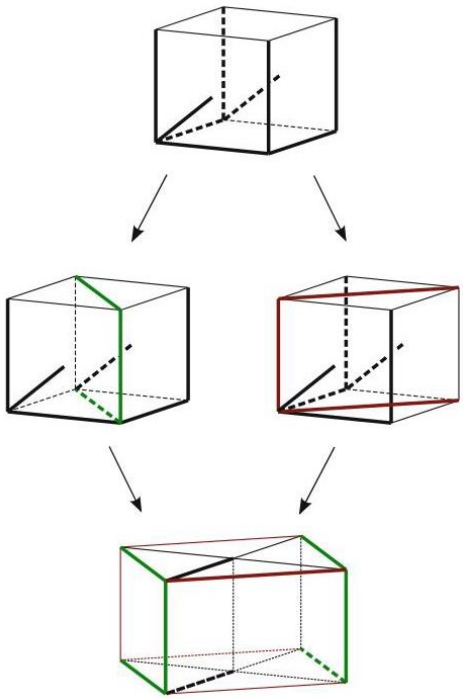

Building on this foundation, the algorithm was extended to non-Abelian lattice gauge theory in [82] and tested successfully for the finite group S_3 . The general procedure is similar to the Abelian case; however, the basis transformations are considerably more complicated as they involve a switch between spin network and holonomy basis via group Fourier transform [77]. Beyond this successful extension of the algorithm to non-Abelian theories, it also underlines two important facts: firstly, the choice of variables, and thus observables described, is crucial in coarse graining algorithms. To preserve the interpretation of the theory, the renormalized theory must be capable of capturing the coarse observables associated with its underlying discretization. To do so, we must choose coarse observables and variables among the original fine ones and adapt the algorithm accordingly to describe these observables. Secondly, for non-Abelian theories, the spin network basis is unstable under coarse graining, as Gauss constraint violations, also known as torsion degrees of freedom, appear from originally gauge invariant amplitudes [58, 83, 84].

在此基础上，文献 [82] 将该算法推广到非阿贝尔格点规范理论，并在有限群 S_3 上通过了测试。整体流程与阿贝尔情形类似，但基变换复杂得多——因为需要通过群傅里叶变换在自旋网络基和和乐基之间切换 [77]。除了成功将算法推广到非阿贝尔理论，这一工作也突显了两个重要事实: 第一，变量的选择 (即所描述的可观测量) 对粗粒化算法至关重要。为保留理论的物理解释，重整化后的理论必须能够捕捉对应基础离散化的粗粒可观测量。为此，我们必须从原细粒变量中选出粗粒可观测量和变量，并相应调整算法来描述这些可观测量。第二，对于非阿贝尔理论，自旋网络基在粗粒化下不稳定，因为原本规范不变的振幅中会出现高斯约束违反，也称为挠率自由度 [58, 83, 84]。

Both aspects are solved by the fusion basis for 3D lattice gauge theory [56,85]. It is a gauge-invariant basis that (a) organizes the degrees of freedom according to a coarse graining (or fusion) scheme and (b) is able to

represent torsion.

三维格点规范理论的融合基解决了这两个问题 [56,85]。它是一种规范不变基，(a) 按照粗粒化 (即融合) 方案组织自由度，(b) 能够表示挠率。

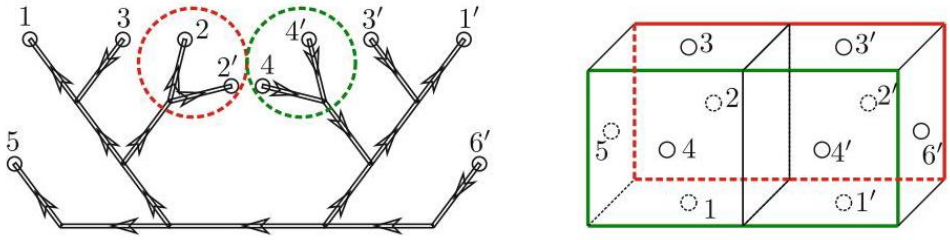

Fig. 6 Choice of fusion tree for coarse graining. The left side shows a fusion tree for two glued 3D cubes. Each end represents an elementary plaquette. The shown fusion tree directly fuses pairs of elementary plaquettes (green and red) into coarse plaquettes

图 6 粗粒化的融合树选择。左侧展示了两个粘合三维立方体的融合树，每个端点对应一个基本元格。图中融合树直接将成对的基本元格 (绿色和红色) 融合为粗粒元格

Consider a 3D cube with six plaquettes. Each plaquette can carry a curvature and torsion excitation. This excitation can be measured by a (generalized) Wilson loop and is characterized by a pair of quantum numbers. Pairs of plaquettes can be fused - correspondingly one can fuse the elementary plaquette excitations. These fused excitations can be again characterized by a pair of quantum numbers, arising from a Wilson loop around the fused plaquettes and so on. This information can be encoded into a (fusion) tree, which has one leave for every elementary plaquette, and carries a pair of quantum numbers on every leave and branch. The quantum numbers are subject to fusion rules, whose precise form depends on the gauge symmetry group.

考虑一个带有六个面块的三维立方体。每个面块都可以承载曲率和挠率激发。这种激发可以通过 (广义) 威尔逊圈测量，并且由一对量子数表征。面块对可以融合——相应地，人们可以融合基本面块激发。这些融合后的激发同样可以由一对量子数表征，量子数来自环绕融合后面块的威尔逊圈，以此类推。这些信息可以编码到一棵 (融合) 树中，树为每个基本面块设置一个叶节点，且每个叶节点和分支都承载一对量子数。量子数满足融合规则，融合规则的具体形式取决于规范对称群。

Gluing cubes to larger blocks, we also glue trees to larger trees. We then apply a tree (i.e., variable) transformation, such that we can fuse the excitations associated with plaquettes to be coarse grained; see Fig. 6. Note that this allows us access to the (coarser) Wilson loop observables around these coarse plaquettes.

将立方体粘合为更大的块时，我们也将树粘合为更大的树。随后我们应用树 (即变量) 变换，从而可以将与面块关联的激发融合，实现粗粒化；参见图 6。请注意，这使得我们能够得到这些粗粒化面块周围的 (更粗粒度的) 威尔逊圈可观测量。

[86] details the construction of a decorated tensor network algorithm for 3D lattice gauge theories with underlying quantum group $SU(2)_k$ symmetry. As outlined the algorithm allows access to coarse-grained Wilson loops. One application is a test of the area law for Wilson loop operators in the strong coupling regime

[86]. The algorithm allows us to identify strong and a weak coupling regimes and the study of how the critical coupling changes as function of the quantum group level k [86].

文献 [86] 详细介绍了针对具有底层量子群 $SU(2)_k$ 对称性的三维格点规范理论，构建装饰张量网络算法的过程。如上所述，该算法可以得到粗粒化威尔逊圈。它的一个应用是在强耦合区对威尔逊圈算符的面积定律进行检验 [86]。该算法可以帮助我们识别强耦合区和弱耦合区，并研究临界耦合如何随量子群级别 k 变化 [86]。

In a nutshell, TNRG-based algorithms are a numerical realization of the consistent boundary formulation implemented and tested for 2D spin net models and 3D models with local Abelian and (q-deformed) non-Abelian gauge symmetry. Embedding maps are derived directly from the amplitudes and define effective coarse degrees of freedom from fine ones depending on their relevance to the dynamics. Strong arguments for TNRG methods are their robust ability to identify different phases of the theory, exploration of the system near phase transitions, and their applicability to models with oscillatory amplitudes. Models with gauge symmetries require special care, due to redundant local variables as well as the instability of spin networks under coarse graining. The fusion basis in 3D is an intriguing solution to these problems.

简而言之，基于 TNRG 的算法是一致边界表述的数值实现，已针对二维自旋网模型和具有局部阿贝尔以及 (q 形变) 非阿贝尔规范对称性的三维模型实现并检验。嵌入映射可直接从振幅导出，根据细粒度自由度对动力学的相关性，由细粒度自由度定义有效的粗粒度自由度。TNRG 方法的突出优点包括: 能稳定识别理论的不同相、探索相变附近的系统，且适用于带有振荡振幅的模型。由于存在冗余局部变量，且粗粒化过程中自旋网络会出现不稳定性，因此处理规范对称模型需要特别注意。三维融合基是解决这些问题的一个令人关注的方案。

Beyond the development of (decorated) tensor network methods for 4D spin foams and lattice gauge theories, spin foams pose additional challenges. Efficient algorithms for evaluating spin foam amplitudes and summing over (fine) degrees of freedom are indispensable. Thanks to progress over the last few years [65,87-93], it is hopefully only a question of time until coarse graining of full 4D spin foams can be tackled. So far, such explorations were only possible by significantly restricting spin foam configurations, which we will detail below.

除了为四维自旋泡沫和格点规范理论开发 (装饰) 张量网络方法之外，自旋泡沫还带来了额外挑战。计算自旋泡沫振幅和对 (细粒度) 自由度求和的高效算法是必不可少的。得益于过去几年的研究进展 [65,87-93]，完整四维自旋泡沫的粗粒化问题有望只是何时能解决的问题。到目前为止，这类探索只能通过大幅限制自旋泡沫构型来实现，我们将在下文详细说明。

Restricted Spin Foam Models

受限自旋泡沫模型

The main idea of restricted spin foam models is to define a subset of the full spin foam path integral. To develop an iterable coarse graining method, it is convenient to choose a 2-complex more general than a triangulation, e.g., one with hypercubic combinatorics. An extension of the Riemannian EPRL model [80] to general 2- complexes was defined in [94]. Instead of summing over all possible shapes of polyhedra, encoded as intertwiners, only specific ones are allowed, typically given by coherent Livine-Speziale intertwiners [95]

peaked on the shape of a classical polyhedron, e.g., a cuboid. Depending on the polyhedron at hand, additional restrictions on the areas of the faces might arise, which furthermore reduce the number of summations in the path integral. In this case, polyhedral restrictions were proposed in [96-99]. Here we will focus on cuboids [96] and frusta [97,98] as these were investigated in the context of renormalization. Cuboids are the 3D analogue of rectangles, where all angles between faces are rectangular and the areas of opposite faces must agree. Eight cuboids are then combined into a hypercuboid, which describes flat spacetime with metric discontinuities and torsion [96]. Frusta on the other hand are 3D generalizations of trapezoids and can be seen as a generalization of the cuboid case. In 4D, two cubes and six frusta form a hyperfrustum, which describes the transition from a cube to a cube of a different size. In Fig. 7, we show how to illustrate the 3D boundary of a hyperfrustum. Therefore this model can be understood as a potential cosmological subsector of spin foam models describing the expansion/contraction of 3D cubulations [97].

受限自旋泡沫模型的核心思想是定义全自旋泡沫路径积分的一个子集。为了开发可迭代的粗粒化方法，选择比三角剖分更一般的 2-复形 (例如具有超立方组合结构的 2-复形) 更为方便。黎曼 EPRL 模型 [80] 到一般 2-复形的推广已在文献 [94] 中给出。该模型不对所有由 intertwiner 编码的多面体可能形状求和，而仅允许特定形状: 这些形状通常由聚集在经典多面体 (例如长方体) 形状附近的相干 Livine-Speziale intertwiner[95] 给出。根据所用多面体的不同，面的面积还会引入额外限制，这会进一步减少路径积分中的求和项数。这类多面体限制已在文献 [96-99] 中提出。本文我们将聚焦于长方体 [96] 和锥台 [97,98]，因为这两类多面体已经在重整化的背景下得到研究。长方体是矩形在三维的类比，其所有面之间的夹角均为直角，且相对面的面积必须相等。八个长方体组合成超长方体，描述带有度量不连续性和挠率的平直时空 [96]。而锥台是梯形在三维的推广，可视为长方体情形的推广。在四维中，两个立方体和六个锥台组成超锥台，描述一个立方体到另一个不同大小立方体的跃迁。图 7 展示了超锥台三维边界的示意图。因此该模型可被理解为自旋泡沫模型中一个潜在的宇宙学子区，描述三维立方剖分的膨胀/收缩 [97]。

The second vital ingredient is the semi-classical approximation of the spin foam amplitudes, in particular the vertex amplitudes. These are hard to compute in the quantum regime, even more so for hypercubic 2-complexes [100]: the vertex amplitude is defined as a contraction of more intertwiners compared to a 4-simplex, and these intertwiners are of a higher valence. The increase in numerical costs is drastic, which makes it impossible to explore the amplitude beyond small spins. While further numerical optimizations are possible, approximating the full vertex amplitude by its semi-classical approximation is indispensable to study coarse graining. The derivation of a semi-classical formula via stationary phase analysis is completely analogous to the 4-simplex case [10,11]. Thanks to using fixed coherent intertwiners, it is straightforward to derive a closed formula for the asymptotic expression of the vertex amplitude. To summarize, intertwiner restrictions and the asymptotic formula for spin foam amplitudes provide readily computable amplitudes as well as restrictions on the configurations to sum over. These drastic simplifications make spin foam model simulations on large 2-complexes with multiple vertices accessible.

第二个关键要素是自旋泡沫振幅 (尤其是顶点振幅) 的半经典近似。这些振幅在量子 regime 难以计算，超立方 2-复形的情形更是如此 [100]: 与 4-单形相比，顶点振幅定义为更多 intertwiner 的缩并，且这些 intertwinner 的价数更高。数值计算成本会大幅飙升, 导致无法研究小自旋之外的振幅。尽管还可以进一步做数值优化，用半经典近似近似全顶点振幅对于研究粗粒化而言是必不可少的。通过稳相近似推导半经典公式的过程与 4-单形的情形完全类似 [10,11]。由于采用固定相干 intertwiner, 可以很方便地推导出顶点振幅渐近表达式的闭合公式。总而言之，intertwiner 限制与自旋泡沫振幅的渐近公式既提供了易于计算的振幅，也对需要求和的构型做了限制。这些大幅简化使得在包含多个顶点的大 2-复形上进行自旋泡沫模型模拟成为可能。

Fig. 7 The 3D boundary of a hyperfrustum: two 3D cubes of different sizes are connected to each other via six 3D frusta, generalizations of trapezoids

图 7 超锥台的三维边界: 两个大小不同的三维立方体通过六个三维锥台 (梯形的三维推广) 相互连接

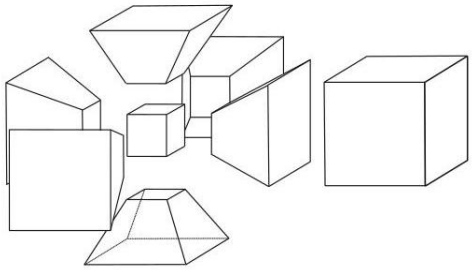

After this basic outline on the definition of the model, let us briefly explain the coarse graining method as it uses the ideas of the consistent boundary formulation, yet employs further approximations to derive a renormalization group flow. Again, embedding maps are used to relate boundary Hilbert spaces, e.g., the one of a subdivided hypercuboid to the Hilbert space of a coarse hypercuboid. These embedding maps are, however, not dynamical and instead geometrically motivated. Take again the example of a hypercuboid: a refined hypercuboid, consisting of 16 hypercuboids, gives rise to a coarse hypercuboid, whose square areas are given by the total area of the subdivided squares. Hence, a coarse hypercuboid amplitude is defined as a superposition of all refined amplitudes giving rise to this coarse geometry.

在完成模型定义的基本概述后，我们来简要解释粗粒化方法: 该方法采用一致边界公式的思想，但使用了额外的近似来导出重整化群流。同样，嵌入映射被用来关联边界希尔伯特空间，例如，将细分超长方体的边界希尔伯特空间与粗粒化超长方体的希尔伯特空间关联起来。但这些嵌入映射不是动力学的，而是由几何动机驱动的。仍以超长方体为例: 一个由 16 个超长方体组成的精细超长方体，可以对应一个粗粒化超长方体，后者的正方形面积等于细分后所有正方形的总面积。因此，粗粒化超长方体振幅定义为所有产生该粗粒几何的精细振幅的叠加。

In contrast to TNRG methods, the amplitude itself is not used to derive the renormalization group flow; instead we compare expectation values of observables for a coarse and fine 2-complex while keeping the boundary data fixed, such that we represent the same transition in both cases. These expectation values are computed by numerical integration techniques [101]. For the results to agree and the theory to give consistent predictions, we must adapt the parameters in the coarse and fine cases. If the expectation values (approximately) match, the coarse amplitude can be understood as the effective description of the fine one, which defines a renormalization group flow of the amplitudes projected onto the original parametrization of the

amplitude. Because of this projection, this method washes out details of the renormalized amplitude. Therefore, as for other renormalization methods, we obtain a flow under certain assumptions and truncations, which necessarily must be eventually lifted to check its viability.

与 TNRG 方法不同，振幅本身并不用于导出重整化群流；相反，我们在固定边界数据的前提下，比对粗化和精细化 2 复形上可观测量的期望值，这样就能保证两种情况描述的是同一个跃迁。这些期望值通过数值积分技术计算得到 [101]。为了让结果一致、理论给出自洽的预言，我们必须调整粗化和精细化情形下的参数。如果期望值 (近似) 匹配，就可以将粗化振幅视为精细化振幅的有效描述，由此就定义了投影到振幅原参数化下的振幅重整化群流。由于这一投影操作，该方法会抹除重整化后振幅的细节。因此，和其他重整化方法一样，我们是在特定假设和截断下得到流，最终必须放开这些假设与截断才能检验流的可行性。

For the renormalization group flow studied for cuboids [44,102] and frusta [103], one parameter plays a crucial role, the exponent of the face amplitude. It is added by hand to reflect an ambiguity in the definition of the EPRL model (This ambiguity can be fixed by demanding invariance of the face amplitude under subdivisions of the faces [104].) without changing the overall form of the amplitude and can be seen as a modification of the path integral measure. In the cuboid case, the face amplitude can be translated into (a certain power of) the volume of a hypercuboid. A similar path integral measure has been discussed in quantum Regge calculus [105]. This exponent has a strong effect on the scaling behavior of the amplitude affecting in the renormalization group flow: for both cuboids and frusta indications for a UV-attractive fixed point were found, which indicates a second-order phase transition. Indeed, this might be related to a restoration of (an Abelian subgroup of) diffeomorphisms. Furthermore, in the frusta setting, the parameter space included gravitational and cosmological constants, which might be related to UV-repulsive directions (for the transitions considered). Further research, in particular lifting of the assumptions mentioned above, is necessary to show whether these results are robust.

在长方体 [44,102] 和台形 [103] 情形下研究的重整化群流中，有一个参数起到关键作用，那就是面振幅的指数。它是手动添加的，用来反映 EPRL 模型定义中的一种歧义 (可以要求面振幅在面细分下不变来消除这种歧义 [104])，同时不改变振幅的整体形式，可将其视为对路径积分测度的修正。在长方体情形下，面振幅可以转化为超长方体体积的某次幂。量子里奇微积分中也讨论过类似的路径积分测度 [105]。该指数对振幅的标度行为有显著影响，进而影响重整化群流: 长方体和台形情形都找到了紫外吸引不动点的迹象，这说明存在二级相变。这实际上可能和微分同胚 (的一个阿贝尔子群) 的恢复有关。此外，在台形框架下，参数空间包含引力常数和宇宙学常数，二者可能和 (所研究跃迁的) 紫外排斥方向相关。要证明这些结果的可靠性，还需要进一步研究，尤其是放开上文提到的假设。

In addition to coarse graining calculations, the restricted spin foam models additionally opened the door toward exploring observables on such quantum spacetimes, e.g., the spectral dimension [106] and spin foam matter systems [107]. However, while these first insights are valuable, the restrictions on the spin foam path integral must eventually be lifted. Unfortunately, the large numerical costs in the quantum regime [100] are an obstacle, which is less pronounced for triangulations. An interesting approach, which picks up the idea to utilize the semiclassical approximation of the vertex amplitude while barely restricting the path integral, is effective spin foam models.

除了粗粒化计算之外，约束自旋泡沫模型还为探索这类量子时空上的可观测量打开了大门，例如谱维 [106] 和自旋泡沫物质系统 [107]。不过，尽管这些初步见解很有价值，对自旋泡沫路径积分的约束最终还是要放开。遗憾的是，量子区域的高昂数值成本 [100] 是一大阻碍，这一问题在三角剖分中没有这么突出。有效自旋泡沫模型是一种很有吸引力的方案，它继承了利用顶点振幅半经典近似的思路，同时几乎不对路径积分附加约束。

Effective Spin Foam Models and Their Refinement Limit

有效自旋泡沫模型及其精化极限

The various methods for determining the renormalization flow via iterative coarse graining and refining require some control on the dynamics of the underlying discrete theory. Spin foam models on the other hand have complex and complicated amplitudes, making the assessment of spin foam dynamics difficult even for quite coarse triangulations. Although there have been recent improvements of numerical techniques for spin foams [65, 87, 88, 92, 108] , the amount of numerical resources required remains challenging.

通过迭代粗粒化和精化确定重整化流的各类方法，都需要对底层离散理论的动力学进行一定控制。而自旋泡沫模型的振幅非常复杂，即使对于相当粗糙的三角剖分，也难以评估自旋泡沫动力学。尽管最近自旋泡沫的数值技术已有改进 [65, 87, 88, 92, 108] ，但所需的数值资源量仍然颇具挑战。

Recently, a new family of gravitational spin foam models, which go by the name ”effective spin foams,” has been constructed in [89, 90, 109]. These new models have numerically accessible amplitudes with a transparent structure, while keeping the universal dynamical properties of spin foams. This has allowed unprecedented computations of expectation values [90] and surprising insights into the dynamics of the refinement limit [110]. In what follows, we discuss effective spin foams and their (perturbative) refinement limit.

近年来，研究者在文献 [89, 90, 109] 中构建了一类新的引力自旋泡沫模型，称为“有效自旋泡沫”。这些新模型的振幅结构清晰、可通过数值计算，同时保留了自旋泡沫的普适动力学性质。这使得研究者能够进行前所未有的期望值计算 [90]，并对精化极限的动力学获得了惊人的洞见 [110]。下文我们将讨论有效自旋泡沫及其 (微扰) 精化极限。

Like all spin foam models, effective spin foams are path integrals over quantum geometries, derived from loop quantum gravity, and associated with triangulations. Such geometries can be labeled by the discrete eigenvalues for the areas in the triangulation. One has furthermore so-called intertwiner labels encoding the quantum shape of the tetrahedra [6]. In effective spin foams, these are assumed to be integrated out for the bulk tetrahedra. This does reduce the number of degrees of freedom considerably and provides one reason for the numerical efficiency of the models.

和所有自旋泡沫模型一样，有效自旋泡沫是源自圈量子引力的量子几何路径积分，与三角剖分相关联。这类几何可以由三角剖分中面积的离散本征值标记。此外还有所谓交缠子标记，用来编码四面体的量子形状 [6]。在有效自旋泡沫中，我们假设 bulk 四面体的交缠子已经被积掉。这大幅减少了自由度，也是该模型数值高效的原因之一。

Spin foam construction is based on an extended configuration space, which is shared by a topological

field theory. The latter fact allows an exact quantization of this extended configuration space [5]. To obtain gravity one has to implement simplicity constraints, which reduce the extended configuration space to the one of (length) metric degrees of freedom. Part of these simplicity constraints are, however, second class [5, 111]. This prevents a sharp implementation of this part of the constraints, which is therefore imposed only weakly, but as strongly as allowed by the non-commutativity of the constraints. This non-commutativity is parametrized by the Barbero-Immirzi parameter [112, 113], which acts therefore as anomaly parameter, controlling fluctuations away from (length) metricity [114].

自旋泡沫的构建基于一个拓展构型空间，拓扑场论也共享这一空间。这一特性使得该拓展构型空间可以被精确量子化 [5]。要得到引力，我们必须施加简单性约束，将拓展构型空间约化为 (长度) 度量自由度。但这些约束的一部分是第二类约束 [5, 111]。这导致约束的这一部分无法严格施加，因此只能弱施加，但满足约束不对易性允许的最强施加条件。这种不对易性由巴贝罗-伊米尔齐参数参数化 [112, 113]，因此该参数充当反常参数，控制偏离 (长度) 度量性的涨落 [114]。

As mentioned above, in effective spin foams the bulk intertwiner degrees of freedom are integrated out. This leaves us with the second class part of the constraints in terms of the area variables only (That the constraints are second class follows also from the discreteness of the area spectra and the polynomial nature of the constraints. In terms of the area eigenvalues, the constraints appear as diophantine equations, which have too few solutions to allow for a semi-classical regime [89].). The constraints can be localized to pairs of neighboring 4-simplices and can thus be associated with the tetrahedra shared by these pairs. For each pair they force the area variables associated with its 16 triangles to arise from a consistent length assignment to its 14 edges. Weak implementation of these constraints leads to Gaussian factors G_τ , whose variances are determined by the anomaly.

如上所述，在有效自旋泡沫中，bulk 交缠子自由度已经被积掉，只剩下仅用面积变量表示的第二类约束 (约束为第二类也可由面积谱的离散性和约束的多项式性质推出: 用面积本征值表示时，约束表现为丢番图方程，其解太少，无法存在半经典区域 [89])。这些约束可以局域到相邻 4-单形对，因此可以关联到这对单形共享的四面体上。对每一对单形，约束要求其 16 个三角形对应的面积变量，都能由 14 条边的一致长度赋值得到。弱施加这些约束会得到高斯因子 G_τ ，其方差由反常确定。

These Gaussian factors make up one part of the effective spin foam amplitudes. The other part is given by the exponential (Other choices, like the cosine of the Regge action, which implements a summation over orientations of the 4-simplices, are also possible [115, 116]) of the area Regge action S_A . In summary, the effective spin foam amplitudes take the simple form

这些高斯因子构成了有效自旋泡沫振幅的一部分，另一部分由面积里奇作用的指数给出 (也可以采用其他选择，例如实现 4-单形取向求和的里奇作用余弦，这同样可行 [115, 116])) 面积里奇作用 S_A 。综上，有效自旋泡沫振幅可写成如下简单形式

$$Z = \sum_{\{a\}} \mu(a)\, e^{\imath S_A(a)} \prod_\tau G_\tau(a) \tag{18}$$

where $\mu(a)$ is a measure factor to be fixed, for example, by demanding discretization invariance [32].

其中 $\mu(a)$ 是待固定的测度因子，例如可以通过要求离散化不变性来固定 [32]。

Similar to the construction of previous spin foam models from gauge theoretic topological quantum field theories, effective spin foams can be motivated from higher gauge theory, where the exponential of the Regge action appears directly (and not only as semi-classical limit) as an amplitude of a related topological quantum field theory [117-119]. Note that the EPRL/FK models [80, 120] can be cast into a form similar to (18), that is, as state-sums of products of oscillating vertex amplitudes and products of terms enforcing gluing conditions between vertices [121].

和此前从规范理论拓扑量子场论构建自旋泡沫模型类似，有效自旋泡沫可以从高规范理论得到动机: 在高规范理论中，里奇作用的指数直接作为相关拓扑量子场论的振幅出现 (而非仅作为半经典极限)[117-119]。注意 EPRL/FK 模型 [80, 120] 也可以写成和 (18) 类似的形式，即作为振荡顶点振幅乘积与顶点间粘合条件项乘积的状态和 [121]。

The numerical accessibility of effective spin foams has been leveraged to elucidate the so-called flatness problem [122, 123]. Their transparent form of the dynamics has allowed a perturbative analysis of the refinement limit [110]. In the following, we will shortly review these results.

有效自旋泡沫的数值可及性已经被用于阐明所谓平坦性问题 [122, 123]。其清晰的动力学形式使得我们可以对精化极限进行微扰分析 [110]。下文我们将简要综述这些结果。

Discrete Gravity Dynamics from Semi-classical Limit

来自半经典极限的离散引力动力学

The study of the semi-classical limit of spin foams [8, 10, 11, 124] , i.e., of the limit $\hbar \to 0$ (For spin foams, this is the limit of large areas associated with the triangles in the triangulation.), has revealed that configurations with non-vanishing curvature are suppressed [123]. This suggested that spin foams might not lead to general relativity and became known as ”flatness problem” [65, 122, 123, 125-127].

对自旋泡沫 [8, 10, 11, 124] 的半经典极限，即极限 $\hbar \to 0$ (对自旋泡沫而言，该极限指三角剖分中三角形对应大面积的极限) 的研究表明，非零曲率构型会被压制 [123]。这说明自旋泡沫可能无法导出广义相对论，该问题被称为“平坦性问题”[65, 122, 123, 125-127]。

Although the flatness problem has been first identified for EPRL/FK models, it has been shown that it is a generic (A second more technical requirement is that the action is not stationary along the gradient of the constraints. Thus, examples where second class constraints are used for gauge fixing constant directions in the action avoid this problem.) feature for path integrals with weakly imposed constraints [89, 90]. As the need for weakly imposed constraints follows from the discreteness of the area spectra [89], one has to expect a version of the flatness problem for all models with discrete (and approximately equidistant) area spectra.

虽然平坦性问题最初是在 EPRL/FK 模型中发现的，但已被证明它是带弱施加约束的路径积分的通用性质 (第二个更技术性的条件是作用量沿约束梯度不平稳，因此，使用二类约束固定作用量中常数方向规范的例子可以避免该问题)[89, 90]。由于面积谱的离散性决定了必须引入弱施加约束 [89]，因此可以预期所有带离散 (且近似等距) 面积谱的模型都存在某一版本的平坦性问题。

But with the insight that the flatness problem results from an anomalous constraint algebra arises a resolution, namely, that together with the $\hbar \to 0$ limit, one also has to take the anomaly parameter, thus the Barbero-Immirzi parameter, to be small [90,128]. Now, as the Barbero-Immirzi parameter does control the spectral gap for spatial areas [45, 129, 130] , one would like to know how small the Barbero-Immirzi parameter has to be, in order to allow for a semi-classical regime with gravitational equations of motion.

但认识到平坦性问题源于反常约束代数后，就找到了一个解决方案: 在取 $\hbar \to 0$ 极限的同时，还必须让反常参数 (即巴贝罗-伊米里齐参数) 趋近于小量 [90,128]。既然巴贝罗-伊米里齐参数确实控制着空间面积的谱隙 [45, 129, 130] ，我们需要知道巴贝罗-伊米里齐参数需要多小，才能允许存在满足引力运动方程的半经典区域。

The computational advantages of effective spin foams allowed the first explicit computation [90] of geometric expectation values for a triangulation, sufficiently large to test the equations of motion. The results have shown that (effective) spin foams do implement a discrete version of the Einstein equations. The range of allowed parameters is larger than suggested by simple scaling arguments [90, 128] and includes, even for large curvature of the classical solutions, Barbero-Immirzi parameters as large as $\sim 0.1 - 0.2$. This range includes values, which are suggested by black hole state counting [131-134].

有效自旋泡沫的计算优势使得研究者首次对三角剖分的几何期望值完成了显式计算 [90]，该三角剖分足够大, 可以检验运动方程。结果表明, (有效) 自旋泡沫确实实现了爱因斯坦方程的离散形式。允许参数的范围比简单标度论证预测的更大 [90, 128]，即使对经典解的大曲率情形，允许的巴贝罗-伊米里齐参数最大可达 $\sim 0.1 - 0.2$ 。这个范围也包含黑洞态计数给出的参数值 [131-134]。

This has resolved the flatness problem for small triangulations. One might however ask whether the flatness problem reappears for triangulations with many building blocks. Considering larger and larger triangulations, we have more and more degrees of freedom describing fluctuations away from length metric configurations. These might turn out to dominate in the refinement limit.

这就解决了小三角剖分的平坦性问题。但我们仍然可以提问: 在包含大量构造块的三角剖分中，平坦性问题是否会再次出现? 当三角剖分越来越大时，我们拥有越来越多的自由度，用来描述偏离长度度量构型的涨落。这些涨落在精细化极限中可能会占据主导。

The Perturbative Refinement Limit of Spin Foams

自旋泡沫的微扰精化极限

Ignoring the measure term, we can extract from the effective spin foam amplitude (18) an action

忽略测度项，我们可以从有效自旋泡沫振幅 (18) 中提取出一个作用量

$$S = S_A(a) - \imath \sum_\tau \ln G_\tau(a). \tag{19}$$

The works [110, 135] assume that one can apply the background field method to effective spin foams and therefore considers an expansion of the action (19) around a flat solution. More precisely, one considers

triangulations with the symmetries of the hypercubical lattice, embedded into flat space. This embedding of a hypercubical lattice comes with two parameters, namely, the lattice constant (defined by the background lengths of the edges of the hypercubes) and the number N^4 of hypercubes in the lattice. Choosing N large, we can consider fluctuations with a large wavelength as compared to the lattice constant. Truncating the action to quadratic order in the fluctuations, we can apply a lattice Fourier transform, and fluctuations of different wavelengths will not interact with each other.

文献 [110, 135] 假设背景场方法可应用于有效自旋泡沫，因此考虑将作用量 (19) 围绕平直解展开。更准确地说，所考虑的三角剖分具有超立方格点的对称性，嵌入在平直空间中。这种超立方格点的嵌入包含两个参数，即格点常数 (由超立方体边的背景长度定义) 和格点中超立方体的数量 N^4 。选择较大的 N 时，我们可以研究波长比格点常数大很多的涨落。将作用量截断到涨落的二次阶，我们可以应用格傅里叶变换，不同波长的涨落之间不会发生相互作用。

In the refinement (or continuum) limit we consider the dynamics at wavelengths much larger than the lattice constant. Here it is important to identify terms in the action, which have a homogeneous scaling in the lattice constant. Such terms can be identified after applying a variable transformation to a set of variables that describe an area metric. An area metric [136] measures the areas of parallelograms in the tangent space. It has 20 components as compared to the 10 components of the length metric. One can however define a length metric from an area metric [137] and thus split the area metric into length metric and non-length-metric degrees of freedom.

在精化 (即连续) 极限下，我们研究波长远大于格点常数的动力学。这里关键是识别出作用量中随格点常数均匀标度的项，这类项可以在对描述面积度规的变量组做变量变换后得到。面积度规 [136] 测量切空间中平行四边形的面积。和长度度规的 10 个分量相比，面积度规有 20 个分量。不过我们可以从面积度规定义出长度度规 [137]，从而将面积度规拆分为长度度规自由度和非长度度规自由度。

The action for the length metric degrees of freedom is of zeroth order in the lattice constant and provides the dominant part in the continuum limit. This action agrees with the linearized Einstein-Hilbert action. Integrating out the non-length-metric degrees of freedom, one finds a subleading correction (at quadratic order in the lattice constant) to the Einstein-Hilbert action [110]. This correction is given by the square of the (linearized) Weyl curvature and arises because of the extension of the configuration space from length to area variables.

长度度规自由度对应的作用量是格点常数的零阶项，是连续极限下的主导部分，该作用量与线性化爱因斯坦-希尔伯特作用量一致。积去非长度度规自由度后，我们会得到爱因斯坦-希尔伯特作用量的次领头修正 (格点常数的二次阶)[110]，该修正由 (线性化) 外尔曲率的平方给出，其起源是构型空间从长度变量扩展到了面积变量。

This behavior is explained by the fact that the length metric degrees of freedom are massless (the part of the action quadratic in these variables is also quadratic in derivatives), whereas the non-length-metric degrees of freedom come with a mass, determined by the lattice constant. Thus, these non-length-metric degrees of freedom essentially localize onto regions with size of a few lattice constants. Surprisingly, the dynamics of the area Regge action itself provides such mass terms - one actually does not need the constraint terms in (19). Adding these constraint terms, one does affect the mass terms, but it does not change the structure of the results [135].

这一特性可以用以下事实解释: 长度度规自由度是无质量的 (作用量中这些变量的二次项同时也是导数的二次项)，而非长度度规自由度带有由格点常数决定的质量。因此，这类非长度度规自由度本质上局域在几个格点常数大小的区域内。令人惊讶的是，面积里奇作用量本身的动力学就给出了这类质量项——实际上 (19) 中的约束项并不是必需的。添加这些约束项确实会改变质量项，但不会改变结果的结构 [135]。

As the various spin foam models differ in the details of their constraint implementation, these results hint at a universality mechanism that arises in the continuum limit. This is confirmed by an analysis that starts directly with the continuum field theory, underlying spin foam construction, namely, the Plebanski action [7]. The weak implementation of the constraints can be modeled by a modified Plebanski action [138, 139], where the constraints are replaced by mass terms. Using this approach one can model the extension of the length metric configuration space to an area metric configuration space [137]. Integrating out the non-length-metric degrees of freedom one finds again the Einstein-Hilbert action with a correction, given by the square of the Weyl curvature [137].

由于不同自旋泡沫模型的约束实现细节各不相同，上述结果暗示连续极限下存在一种普适机制。这一点已经得到分析验证，该分析直接从自旋泡沫构造 underlying 的连续场论即普莱班斯基作用量 [7] 出发。弱约束可以用修改后的普莱班斯基作用量建模 [138, 139]，其中原约束被替换为质量项。使用该方法我们可以对长度度规构型空间到面积度规构型空间的扩展建模 [137]。积去非长度度规自由度后，我们仍会得到带有外尔曲率平方修正的爱因斯坦-希尔伯特作用量 [137]。

To summarize, effective spin foams have in particular allowed to probe the aspects of spin foam dynamics, which arise from the extension of the configuration space of length (metric) variables. Applying a ”naive” semi-classical limit $\hbar \to 0$, this extension leads to the so-called flatness problem. This issue can be resolved by recognizing that the Barbero-Immirzi parameter is an anomaly parameter and has to be chosen to scale with $\hbar$ for a proper semi-classical limit. Explicit computations of expectation values in effective spin foams have identified semi-classical regimes with a gravitational dynamics, allowing for finite small values of $\hbar$ and the Barbero-Immirzi parameter [90]. One can furthermore consider a perturbative continuum limit [110, 135]. This reveals that all the non-length-metric degrees are massive, whereas the length metric degrees of freedom are massless. Thus, in the continuum limit, the non-length-metric degrees of freedom are suppressed. This provides a mechanism for resolving the flatness problem in the continuum limit, which works for arbitrary values of the Barbero-Immirzi parameter.

总而言之，有效自旋泡沫尤其允许我们探究自旋泡沫动力学中，由长度 (度规) 变量构型空间扩展带来的特性。应用“朴素”半经典极限 $\hbar \to 0$ ，这种扩展会导致所谓的平直性问题。该问题可以通过下述结论解决: 巴贝罗-伊米尔齐参数是一个反常参数，要得到合适的半经典极限，它必须随 $\hbar$ 标度。有效自旋泡沫中期望值的显式计算已经识别出存在引力动力学的半经典区域，该区域允许 $\hbar$ 和巴贝罗-伊米尔齐参数取有限小值 [90]。我们还可以进一步考虑微扰连续极限 [110, 135]，结果表明所有非长度度量自由度都是有质量的，而长度度规自由度是无质量的。因此在连续极限下，非长度度规自由度被压低，这就提供了一种连续极限下解决平直性问题的机制，该机制对任意巴贝罗-伊米尔齐参数取值都成立。

The lattice techniques developed in [110, 135] may also allow to extract a renormalization flow for the perturbative effective action, along the lines of [25].

文献 [110, 135] 中发展的格点技术，也可以遵循文献 [25] 的思路，用于提取微扰有效作用量的重整化流。

Concluding Remarks

结束语

Gravitational spin foams are defined on triangulations, which act as regulator in their path integral construction. This makes spin foams regulator (i.e., triangulation) dependent. It furthermore breaks diffeomorphism symmetry and introduces many unwanted ambiguities. We have argued that all these issues can be resolved, if one constructs improved and perfect actions. Such actions lead however to nonlocal couplings, which are difficult to handle in particular for the spin foam framework. Nonlocal couplings are avoided in the consistent boundary formalism. It provides a renormalization framework that serves to construct consistent (i.e., regulator independent) amplitudes in background independent theories such as spin foams, for spacetime regions with more and more complex boundary data. To implement this in practice, one has to choose truncations. Importantly the consistent boundary framework allows to identify truncations that are adapted to the dynamics such that they minimize the induced error for the evaluation of the partition function. Tensor network coarse graining provides concrete algorithms that can be used to implement the consistent boundary framework. Originally constructed for 2D systems, they needed to be improved and modified to allow applications to higher-dimensional systems with gauge symmetries. In particular, decorated tensor networks have been successfully applied to 3D non-Abelian lattice gauge systems, emulating spin foams.

引力自旋泡沫定义在三角剖分上，三角剖分在其路径积分构造中充当正则化器。这使得自旋泡沫依赖于正则化器 (即三角剖分)。它还会破坏微分同胚对称性，并引入许多不必要的歧义。我们已经论证，若构造改进的完美作用量，所有这些问题都可以得到解决。但这类作用量会导致非定域耦合，这类耦合尤其难以在自旋泡沫框架中处理。非定域耦合可以在一致边界形式中避免，该形式提供了一个重整化框架，可用于在自旋泡沫这类背景无关理论中，为边界数据越来越复杂的时空区域构造一致 (即不依赖正则化器) 的振幅。要实际实现这一点，我们必须选择截断。重要的是，一致边界框架可以识别适配动力学的截断，从而将配分函数计算中的诱导误差降到最低。张量网络粗粒化提供了可用于实现一致边界框架的具体算法。这类算法最初为二维系统构造，需要进行改进和修改才能应用于带有规范对称性的高维系统。特别是装饰张量网络已经成功应用于模拟自旋泡沫的三维非阿贝尔格点规范系统。

Applying such coarse graining algorithms to the 4D gravitational spin foam models remains an enormous computational challenge. This is in no small part due to the complexity of the spin foam amplitudes. We presented two approaches that lead to a simplification of the amplitudes (which can also be combined). Restricted spin foams combine a symmetry reduction of degrees of freedom with semiclassical approximations. This has allowed to derive a renormalization flow, which illustrated the restoration of a partial set of diffeomorphism symmetries at the fixed point. Effective spin foams are much more accessible to numerical computations than traditional models and offer a transparent encoding of the dynamics. These features can be leveraged to show that the flatness problem, which seemed to endanger a suitable semi-classical limit for spin foams, can be resolved both on the discrete level and in the refinement limit.

将这类粗粒化算法应用于四维引力自旋泡沫模型仍然是一项巨大的计算挑战，这在很大程度上源于自旋泡沫振幅本身的复杂性。我们提出了两种可简化振幅的方法 (也可组合使用)。受限自旋泡沫将自由度的对称性约化与半经典近似结合，这使得我们可以推导出重整化流，表明在不动点处会恢复部分微分同胚对称性。有效自旋泡沫比传统模型更易于数值计算，还能清晰地编码动力学。利用这些特性可以证明，一度被认为会威胁自旋泡沫获得合适半经典极限的平坦性问题，在离散层面和精化极限下都可以得到解决。

In particular, effective spin foams allowed for a perturbative refinement limit. This is described by the Einstein-Hilbert action and a Weyl squared curvature term. The latter arises from a key feature of spin foams, namely, the extension of the underlying configuration space from length to area metrics. Although this extension is forced from the discrete area spectra of loop quantum gravity, we should note that the found action does not capture directly the effects resulting from these discrete spectra.

特别是，有效自旋泡沫允许存在微扰精化极限，该极限由爱因斯坦-希尔伯特作用量和外尔平方曲率项描述。后者来源于自旋泡沫的一个核心特征，即其基础构型空间从长度度量扩展到了面积度量。尽管这种扩展是圈量子引力离散面积谱所要求的，但我们需要指出，我们得到的作用量并没有直接涵盖这些离散谱带来的效应。

In closing, we remark that many questions about the non-perturbative refinement limit remain open. Spin foams feature many degenerate configurations, e.g., so-called vector geometries [10, 11, 87, 88] , that might turn out to dominate in the limit. This holds even more so for Lorentzian signature models [140-142]. In addition, Lorentzian models can also feature topology change, e.g., generation of baby universes [91, 109]. Luckily, effective spin foams allow for an easier control of such configurations.

最后我们要说明，关于非微扰精化极限的许多问题仍然没有解决。自旋泡沫存在大量简并构型，例如所谓的向量几何 [10, 11, 87, 88] ，这些构型可能会在极限中占据主导。这种情况在洛伦兹号差模型中更为突出 [140-142]。此外，洛伦兹模型还可能存在拓扑变化，例如婴儿宇宙的产生 [91, 109]。幸运的是，有效自旋泡沫可以更轻松地控制这类构型。

Many non-perturbative (Euclidean) lattice approaches suffer from the conformal factor problem [13]. This leads, in, e.g., Regge calculus, to an abundance of spike configurations [143], that is, vertices, where all adjacent edges have (arbitrarily) large lengths. A related problem for spin foams are bubble divergences [144-148]. To achieve a suitable non-perturbative refinement limit, it will be essential to control such divergences. A first step would be to show that spike configurations can be dealt with in Lorentzian quantum Regge calculus.

许多非微扰 (欧氏) 格点方法都存在共形因子问题 [13]。例如在里奇微积分中，这会导致产生大量尖峰构型 [143]，即所有邻边长度都 (任意) 很大的顶点。自旋泡沫中一个相关问题是泡泡发散 [144-148]。要获得合适的非微扰精化极限，控制这类发散至关重要。第一步可以先证明尖峰构型可以在洛伦兹量子里奇微积分中得到处理。

Cross-References

交叉引用

Emergence of Riemannian Quantum Geometry

黎曼量子几何的出现

- Hamiltonian Theory: Dynamics

  - 哈密顿理论: 动力学

Spin Foams: Foundations

自旋泡沫: 基础

Spinfoams and High-Performance Computing

自旋泡沫与高性能计算

The Functional Renormalization Group in Quantum Gravity

量子引力中的泛函重整化群

Acknowledgments BD and SSt appreciate deeply many discussions and collaborations with Benjamin Bahr on the topics discussed here. Research at Perimeter Institute is supported in part by the Government of Canada through the Department of Innovation, Science and Economic Development Canada and by the Province of Ontario through the Ministry of Colleges and Universities. SKA is supported by the Alexander von Humboldt foundation. SSt gratefully acknowledges support by the Deutsche Forschungsgemeinschaft (DFG, German Research Foundation) - Projektnummer/project-number 422809950.

致谢 BD 与 SSt 非常感谢与 Benjamin Bahr 就本文讨论的主题开展的诸多讨论与合作。周边理论物理研究所的研究部分得到加拿大政府通过加拿大创新、科学与经济发展部，以及安大略省通过大专与大学部的资助。SKA 得到亚历山大·冯·洪堡基金会的支持。SSt 衷心感谢德国研究基金会 (DFG) 的资助——项目编号 422809950。

References

参考文献

1. T. Regge, General relativity without coordinates. Nuovo Cim. 19, 558-571 (1961)

2. J.W. Barrett, M. Rocek, R.M. Williams, A note on area variables in Regge calculus. Class. Quant. Grav. 16, 1373-1376 (1999). http://arxiv.org/abs/gr-qc/9710056, arXiv:gr-qc/9710056

3. B. Dittrich, S. Speziale, Area-angle variables for general relativity. New J. Phys. 10, 083006 (2008). http://arxiv.org/abs/0802.0864, arXiv:0802.0864 [gr-qc]

4. J.C. Baez, An introduction to spin foam models of quantum gravity and BF theory. Lect. Notes Phys. 543, 25-94 (2000). http://arxiv.org/abs/gr-qc/9905087, arXiv:gr-qc/9905087

5. A. Perez, The spin foam approach to quantum gravity. Living Rev. Rel. 16, 3 (2013). http:// arxiv.org/abs/1205.2019, arXiv:1205.2019 [gr-qc]

6. J.C. Baez, J.W. Barrett, The quantum tetrahedron in three-dimensions and four-dimensions. Adv. Theor. Math. Phys. 3, 815-850 (1999). http://arxiv.org/abs/gr-qc/9903060, arXiv:gr-qc/9903060

7. J.F. Plebanski, On the separation of Einsteinian substructures. J. Math. Phys. 18, 2511-2520 (1977)

8. J.W. Barrett, R.M. Williams, The asymptotics of an amplitude for the four simplex. Adv. Theor. Math. Phys. 3, 209-215 (1999). http://arxiv.org/abs/gr-qc/9809032, arXiv:gr-qc/9809032

9. J.C. Baez, J.D. Christensen, G. Egan, Asymptotics of 10j symbols. Class. Quant. Grav. 19, 6489 (2002). http://arxiv.org/abs/gr-qc/0208010, arXiv:gr-qc/0208010

10. F. Conrady, L. Freidel, On the semiclassical limit of 4d spin foam models. Phys. Rev. D 78, 104023 (2008). http://arxiv.org/abs/0809.2280, arXiv:0809.2280 [gr-qc]

11. J.W. Barrett, R. Dowdall, W.J. Fairbairn, H. Gomes, F. Hellmann, Asymptotic analysis of the EPRL four-simplex amplitude. J. Math. Phys. 50, 112504 (2009). http://arxiv.org/abs/0902.1170, arXiv:0902.1170 [gr-qc]

12. M. Rocek, R.M. Williams, Quantum Regge Calculus. Phys. Lett. B 104, 31 (1981)

13. R. Loll, Discrete approaches to quantum gravity in four-dimensions. Living Rev. Rel. 1, 13 (1998). http://arxiv.org/abs/gr-qc/9805049, arXiv:gr-qc/9805049

14. H.W. Hamber, R.M. Williams, Gauge invariance in simplicial gravity. Nucl. Phys. B 487, 345-408 (1997). http://arxiv.org/abs/hep-th/9607153, arXiv:hep-th/9607153

15. P.A. Morse, Approximate diffeomorphism invariance in near flat simplicial geometries. Class. Quant. Grav. 9, 2489 (1992)

16. B. Dittrich, Diffeomorphism symmetry in quantum gravity models. Adv. Sci. Lett. 2(10), 151 (2008). http://arxiv.org/abs/0810.3594, arXiv:0810.3594 [gr-qc]

17. B. Bahr, B. Dittrich, (Broken) gauge symmetries and constraints in Regge calculus. Class. Quant. Grav. 26, 225011 (2009). http://arxiv.org/abs/0905.1670, arXiv:0905.1670 [gr-qc]

18. S.K. Asante, B. Dittrich, H.M. Haggard, The degrees of freedom of area Regge calculus: dynamics, non-metricity, and broken diffeomorphisms. Class. Quant. Grav. 35(13), 135009 (2018). http://arxiv.org/abs/1802.09551, arXiv:1802.09551 [gr-qc]

19. B. Bahr, B. Dittrich, Breaking and restoring of diffeomorphism symmetry in discrete gravity. AIP Conf. Proc. 1196(1), 10 (2009) . http://arxiv.org/abs/0909.5688, arXiv:0909.5688 [gr-qc]

20. B. Bahr, B. Dittrich, S. Steinhaus, Perfect discretization of reparametrization invariant path integrals. Phys. Rev. D 83, 105026 (2011). http://arxiv.org/abs/1101.4775, arXiv:1101.4775 [gr-qc]

21. J.E. Marsden, M. West, Discrete mechanics and variational integrators. Acta Numer. 10, 357- 514 (2001)

22. P. Hasenfratz, F. Niedermayer, Perfect lattice action for asymptotically free theories. Nucl. Phys. B 414, 785-814 (1994). http://arxiv.org/abs/hep-lat/9308004, arXiv:hep-lat/9308004

23. B. Bahr, B. Dittrich, Improved and perfect actions in discrete gravity. Phys. Rev. D 80, 124030 (2009). http://arxiv.org/abs/0907.4323, arXiv:0907.4323 [gr-qc]

24. W. Bietenholz, U.J. Wiese, Perfect lattice actions for quarks and gluons. Nucl. Phys. B 464, 319-352 (1996). http://arxiv.org/abs/hep-lat/9510026, arXiv:hep-lat/9510026

25. B. Bahr, B. Dittrich, S. He, Coarse graining free theories with gauge symmetries: the linearized case. New J. Phys. 13, 045009 (2011). http://arxiv.org/abs/1011.3667, arXiv:1011.3667 [gr-qc]

26. S.K. Asante, B. Dittrich, Perfect discretizations as a gateway to one-loop partition functions for 4D gravity. JHEP 05, 172 (2022). http://arxiv.org/abs/2112.03307, arXiv:2112.03307 [gr-qc]

27. W. Bietenholz, Perfect actions for scalar theories. Nucl. Phys. B Proc. Suppl. 63, 901-903 (1998). http://arxiv.org/abs/hep-lat/9709117, arXiv:hep-lat/9709117

28. T. Lang, K. Liegener, T. Thiemann, Hamiltonian renormalisation I: derivation from Oster-walder-Schrader reconstruction. Class. Quant. Grav. 35(24), 245011 (2018). http://arxiv.org/ abs/1711.05685, arXiv:1711.05685 [gr-qc]

29. T. Lang, K. Liegener, T. Thiemann, Hamiltonian Renormalisation II. Renormalisation Flow of 1+1 dimensional free scalar fields: derivation. Class. Quant. Grav. 35(24), 245012 (2018). http://arxiv.org/abs/1711.06727, arXiv:1711.06727 [gr-qc]

30. T. Lang, K. Liegener, T. Thiemann, Hamiltonian renormalization III. Renormalisation flow of 1 + 1 dimensional free scalar fields: properties. Class. Quant. Grav. 35(24), 245013 (2018). http://arxiv.org/abs/1711.05688, arXiv:1711.05688 [gr-qc]

31. T. Lang, K. Liegener, T. Thiemann, Hamiltonian renormalisation IV. Renormalisation flow of D + 1 dimensional free scalar fields and rotation invariance. Class. Quant. Grav. 35(24), 245014 (2018). http://arxiv.org/abs/1711.05695, arXiv:1711.05695 [gr-qc]

32. B. Dittrich, S. Steinhaus, Path integral measure and triangulation independence in discrete gravity. Phys. Rev. D 85, 044032 (2012). http://arxiv.org/abs/1110.6866, arXiv:1110.6866 [gr-qc]

33. B. Dittrich, W. Kamiński, S. Steinhaus, Discretization independence implies non-locality in 4D discrete quantum gravity. Class. Quant. Grav. 31(24), 245009 (2014). http://arxiv.org/abs/ 1404.5288, arXiv:1404.5288 [gr-qc]

34. B. Dittrich, How to construct diffeomorphism symmetry on the lattice. PoS QGQGS2011, 012 (2011). http://arxiv.org/abs/1201.3840, arXiv:1201.3840 [gr-qc]

35. C. Di Bartolo, R. Gambini, J. Pullin, Canonical quantization of constrained theories on discrete space-time lattices. Class. Quant. Grav. 19, 5275-5296 (2002). http://arxiv.org/abs/ gr-qc/0205123, arXiv:gr-qc/0205123

36. R. Gambini, J. Pullin, Canonical quantization of general relativity in discrete space-times. Phys. Rev. Lett. 90, 021301 (2003). http://arxiv.org/abs/gr-qc/0206055, arXiv:gr-qc/0206055

37. C. Di Bartolo, R. Gambini, R. Porto, J. Pullin, Dirac-like approach for consistent discretiza-tions of classical constrained theories. J. Math. Phys. 46, 012901 (2005). http://arxiv.org/abs/ gr-qc/0405131, arXiv:gr-qc/0405131

38. B. Dittrich, P.A. Hohn, Canonical simplicial gravity. Class. Quant. Grav. 29, 115009 (2012). http://arxiv.org/abs/1108.1
arXiv:1108.1974 [gr-qc]

39. B. Dittrich, P.A. Hoehn, Constraint analysis for variational discrete systems. J. Math. Phys. 54, 093505 (2013). http://arxiv.org/abs/1303.4294, arXiv:1303.4294 [math-ph]

40. B. Dittrich, P.A. Hohn, From covariant to canonical formulations of discrete gravity. Class. Quant. Grav. 27, 155001 (2010). http://arxiv.org/abs/0912.1817, arXiv:0912.1817 [gr-qc]

41. V. Bonzom, B. Dittrich, Dirac's discrete hypersurface deformation algebras. Class. Quant. Grav. 30, 205013 (2013). http://arxiv.org/abs/1304.5983, arXiv:1304.5983 [gr-qc]

42. P.A. Höhn, Quantization of systems with temporally varying discretization I: evolving Hilbert spaces. J. Math. Phys. 55, 083508 (2014). http://arxiv.org/abs/1401.6062, arXiv:1401.6062 [gr-qc]

43. M. Reuter, F. Saueressig, Quantum Gravity and the Functional Renormalization Group: The Road towards Asymptotic Safety (Cambridge University Press, Cambridge 2019), p. 1

44. B. Bahr, S. Steinhaus, Numerical evidence for a phase transition in 4d spin foam quantum gravity. Phys. Rev. Lett. 117(14), 141302 (2016). http://arxiv.org/abs/1605.07649, arXiv:1605.07649 [gr-qc]

45. C. Rovelli, L. Smolin, Discreteness of area and volume in quantum gravity. Nucl. Phys. B 442, 593-622 (1995); [Erratum: Nucl. Phys. B 456, 753-754 (1995)]. http://arxiv.org/abs/gr-qc/9411005, arXiv:gr-qc/9411005

46. C. Rovelli, Discretizing parametrized systems: the magic of Ditt-invariance. http://arxiv.org/ abs/1107.2310, arXiv:1107.2310 [hep-lat]

47. R. Oeckl, A 'General boundary' formulation for quantum mechanics and quantum gravity. Phys. Lett. B 575, 318-324 (2003). http://arxiv.org/abs/hep-th/0306025, arXiv:hep-th/0306025

48. R. Oeckl, General boundary quantum field theory: Foundations and probability interpretation. Adv. Theor. Math. Phys. 12(2), 319-352 (2008). http://arxiv.org/abs/hep-th/0509122, arXiv:hep-th/0509122

49. B. Dittrich, From the discrete to the continuous: towards a cylindrically consistent dynamics. New J. Phys. 14, 123004 (2012). http://arxiv.org/abs/1205.6127, arXiv:1205.6127 [gr-qc]

50. B. Dittrich, The Continuum Limit of Loop Quantum Gravity - A Framework for Solving the Theory (2017), pp. 153-179. http://dx.doi.org/10.1142/9789813220003_0006, http://arxiv.org/abs/1409.1450, arXiv:1409.1450 [gr-qc]

51. A. Ashtekar, C. Isham, Representations of the holonomy algebras of gravity and non-Abelian gauge theories. Class. Quant. Grav. 9, 1433-1468 (1992). http://arxiv.org/abs/hep-th/9202053, arXiv:hep-th/9202053 [hep-th]

52. A. Ashtekar, J. Lewandowski, Projective techniques and functional integration for gauge theories. J. Math. Phys. 36, 2170-2191 (1995). http://arxiv.org/abs/gr-qc/9411046, arXiv:gr-qc/9411046 [gr-qc]

53. T. Thiemann, Modern Canonical Quantum General Relativity (Cambridge University Press, Cambridge, 2008)

54. B. Dittrich, M. Geiller, A new vacuum for Loop Quantum Gravity. Class. Quant. Grav. 32(11), 112001 (2015). http://arxiv.org/abs/1401.6441, arXiv:1401.6441 [gr-qc]

55. B. Bahr, B. Dittrich, M. Geiller, A new realization of quantum geometry. http://arxiv.org/abs/ 1506.08571, arXiv:1506.08571 [gr-qc]

56. B. Dittrich, M. Geiller, Quantum gravity kinematics from extended TQFTs. New J. Phys. 19(1), 013003 (2017). http://arxiv.org/abs/1604.05195, arXiv:1604.05195 [hep-th]

57. T. Thiemann, Quantum spin dynamics (QSD): VII. Symplectic structures and continuum lattice formulations of gauge field theories. Class. Quant. Grav. 18, 3293-3338 (2001). http:// arxiv.org/abs/hep-th/0005232, arXiv:hep-th/0005232

58. B. Dittrich, M. Geiller, Flux formulation of loop quantum gravity: classical framework. Class. Quant. Grav. 32(13), 135016 (2015). http://arxiv.org/abs/1412.3752, arXiv:1412.3752 [gr-qc]

59. B. Dittrich, S. Steinhaus, Time evolution as refining, coarse graining and entangling. New J. Phys. 16, 123041 (2014). http://arxiv.org/abs/1311.7565, arXiv:1311.7565 [gr-qc]

60. M. Levin, C.P. Nave, Tensor renormalization group approach to 2d classical lattice models. Phys. Rev. Lett. 99, 120601 (2007). http://arxiv.org/abs/cond-mat/0611687, arXiv:cond-mat/0611687 [cond-mat]

61. R. Orus, Exploring corner transfer matrices and corner tensors for the classical simulation of quantum lattice systems. Phys. Rev. B 85, 205117 (2012). http://arxiv.org/abs/1112.4101, arXiv:1112.4101 [cond-mat.str-el]

62. B. Dittrich, F.C. Eckert, M. Martin-Benito, Coarse graining methods for spin net and spin foam models. New J. Phys. 14, 035008 (2012). http://arxiv.org/abs/1109.4927, arXiv:1109.4927 [gr-qc]

63. B. Dittrich, S. Mizera, S. Steinhaus, Decorated tensor network renormalization for lattice gauge theories and spin foam models. New J. Phys. 18(5), 053009 (2016). http://arxiv.org/ abs/1409.2407, arXiv:1409.2407 [gr-qc]

64. E. Efrati, Z. Wang, A. Kolan, L.P. Kadanoff, Real-space renormalization in statistical mechanics. Rev. Mod. Phys. 86, 647-667 (2014). http://arxiv.org/abs/1301.6323, arXiv:1301.6323 [cond-mat.stat-mech], https://link.aps.org/doi/10.1103/RevModPhys.86.647

65. F. Gozzini, A high-performance code for EPRL spin foam amplitudes. Class. Quant. Grav. 38(22), 225010 (2021). http://arxiv.org/abs/2107.13952, arXiv:2107.13952 [gr-qc]

66. M. Han, 4-dimensional spin-foam model with quantum Lorentz group. J. Math. Phys. 52, 072501 (2011). http://arxiv.org/abs/1012.4216, arXiv:1012.4216 [gr-qc]

67. W.J. Fairbairn, C. Meusburger, Quantum deformation of two four-dimensional spin foam models. J. Math. Phys. 53, 022501 (2012). http://arxiv.org/abs/1012.4784, arXiv:1012.4784 [gr-qc]

68. H.M. Haggard, M. Han, A. Riello, Encoding curved tetrahedra in face holonomies: phase space of shapes from group-valued moment maps. Ann. Henri Poincare 17(8), 2001-2048 (2016). http://arxiv.org/abs/1506.03053, arXiv:1506.03053 [math-ph]

69. H.M. Haggard, M. Han, W. Kamiński, A. Riello, Four-dimensional Quantum Gravity with a Cosmological Constant from Three-dimensional Holomorphic Blocks. Phys. Lett. B 752, 258-262 (2016). http://arxiv.org/abs/1509.004 arXiv:1509.00458 [hep-th]

70. M. Han, Four-dimensional spinfoam quantum gravity with a cosmological constant: finiteness and semiclassical limit. Phys. Rev. D 104(10), 104035 (2021). http://arxiv.org/abs/2109.00034, arXiv:2109.00034 [gr-qc]

71. V. Turaev, O. Viro, State sum invariants of 3 manifolds and quantum 6j symbols. Topology 31, 865-902 (1992)

72. L.C. Biedenharn, M.A. Lohe, Quantum Group Symmetries and q-Tensor Algebras (World Scientific, Singapore, 1995)

73. B. Dittrich, M. Martin-Benito, S. Steinhaus, Quantum group spin nets: refinement limit and relation to spin foams. Phys. Rev. D 90, 024058 (2014). http://arxiv.org/abs/1312.0905, arXiv:1312.0905 [gr-qc]

74. B. Dittrich, W. Kaminski, Topological lattice field theories from intertwiner dynamics. http:// arxiv.org/abs/1311.1798, arXiv:1311.1798 [gr-qc]

75. B. Dittrich, E. Schnetter, C.J. Seth, S. Steinhaus, Coarse graining flow of spin foam intertwin-ers. Phys. Rev. D 94(12), 124050 (2016). http://arxiv.org/abs/1609.02429, arXiv:1609.02429 [gr-qc]

76. G. Evenbly, G. Vidal, Tensor network renormalization. Phys. Rev. Lett. 115, 180405 (2015). https://link.aps.org/doi/10.

77. B. Bahr, B. Dittrich, J.P. Ryan, Spin foam models with finite groups. J. Grav. 2013, 549824 (2013). http://arxiv.org/abs/1103.6264, arXiv:1103.6264 [gr-qc]

78. B. Dittrich, M. Martín-Benito, E. Schnetter, Coarse graining of spin net models: dynamics of intertwiners. New J. Phys. 15, 103004 (2013). http://arxiv.org/abs/1306.2987, arXiv:1306.2987 [gr-qc]

79. J.W. Barrett, L. Crane, Relativistic spin networks and quantum gravity. J. Math. Phys. 39, 3296-3302 (1998). http://arxiv.org/abs/gr-qc/9709028, arXiv:gr-qc/9709028

80. J. Engle, E. Livine, R. Pereira, C. Rovelli, LQG vertex with finite Immirzi parameter. Nucl. Phys. B 799, 136-149 (2008). http://arxiv.org/abs/0711.0146, arXiv:0711.0146 [gr-qc]

81. S. Steinhaus, Coarse graining spin foam quantum gravity - a review. Front. Phys. 8, 295 (2020). http://arxiv.org/abs/2007.01315, arXiv:2007.01315 [gr-qc]

82. C. Delcamp, B. Dittrich, Towards a phase diagram for spin foams. Class. Quant. Grav. 34(22), 225006 (2017). http://arxiv.org/abs/1612.04506, arXiv:1612.04506 [gr-qc]

83. E.R. Livine, Deformation operators of spin networks and coarse-graining. Class. Quant. Grav. 31, 075004 (2014). http://arxiv.org/abs/1310.3362, arXiv:1310.3362 [gr-qc]

84. E.R. Livine, From coarse-graining to holography in loop quantum gravity. EPL 123(1), 10001 (2018). http://arxiv.org/abs/1704.04067, arXiv:1704.04067 [gr-qc]

85. C. Delcamp, B. Dittrich, A. Riello, Fusion basis for lattice gauge theory and loop quantum gravity. JHEP 02, 061 (2017). http://arxiv.org/abs/1607.08881, arXiv:1607.08881 [hep-th]

86. W.J. Cunningham, B. Dittrich, S. Steinhaus, Tensor network renormalization with fusion charges - applications to 3D lattice gauge theory. Universe 6(7), 97 (2020). http://arxiv.org/ abs/2002.10472, arXiv:2002.10472 [hep-th]

87. P. Doná, M. Fanizza, G. Sarno, S. Speziale, SU(2) graph invariants, Regge actions and polytopes. Class. Quant. Grav. 35(4), 045011 (2018). http://arxiv.org/abs/1708.01727, arXiv:1708.01727 [gr-qc]

88. P. Doná, M. Fanizza, G. Sarno, S. Speziale, Numerical study of the Lorentzian Engle-Pereira-Rovelli-Livine spin foam amplitude. Phys. Rev. D 100(10), 106003 (2019). http://arxiv.org/ abs/1903.12624, arXiv:1903.12624 [gr-qc]

89. S.K. Asante, B. Dittrich, H.M. Haggard, Effective spin foam models for four-dimensional quantum gravity. Phys. Rev. Lett. 125(23), 231301 (2020). http://arxiv.org/abs/2004.07013, arXiv:2004.07013 [gr-qc]

90. S.K. Asante, B. Dittrich, H.M. Haggard, Discrete gravity dynamics from effective spin foams. Class. Quant. Grav. 38(14), 145023 (2021). http://arxiv.org/abs/2011.14468, arXiv:2011.14468 [gr-qc]

91. S.K. Asante, B. Dittrich, J. Padua-Argüelles, Complex actions and causality violations: applications to Lorentzian quantum cosmology. http://arxiv.org/abs/2112.15387, arXiv:2112.15387 [gr-qc]

92. M. Han, Z. Huang, H. Liu, D. Qu, Y. Wan, Spinfoam on a Lefschetz thimble: Markov chain Monte Carlo computation of a Lorentzian spinfoam propagator. Phys. Rev. D 103(8), 084026 (2021). http://arxiv.org/abs/2012.11515, arXiv:2012.11515 [gr-qc]

93. M. Han, Z. Huang, H. Liu, D. Qu, Complex critical points and curved geometries in four-dimensional Lorentzian spinfoam quantum gravity. Phys. Rev. D 106(4), 044005 (2022). http://arxiv.org/abs/2110.10670, arXiv:2110.10670 [gr-qc]

94. W. Kaminski, M. Kisielowski, J. Lewandowski, Spin-foams for all loop quantum gravity. Class. Quant. Grav. 27, 095006 (2010); [Erratum: Class. Quant. Grav. 29, 049502 (2012)]. http://arxiv.org/abs/0909.0939, arXiv:0909.0939 [gr-qc]

95. E.R. Livine, S. Speziale, A new spinfoam vertex for quantum gravity. Phys. Rev. D 76, 084028 (2007). http://arxiv.org/abs/0705.0674, arXiv:0705.0674 [gr-qc]

96. B. Bahr, S. Steinhaus, Investigation of the spinfoam path integral with quantum cuboid intertwiners. Phys. Rev. D 93(10), 104029 (2016). http://arxiv.org/abs/1508.07961, arXiv:1508.07961 [gr-qc]

97. B. Bahr, S. Klöser, G. Rabuffo, Towards a cosmological subsector of spin foam quantum gravity. Phys. Rev. D 96(8), 086009 (2017). http://arxiv.org/abs/1704.03691, arXiv:1704.03691 [gr-qc]

98. B. Bahr, G. Rabuffo, Deformation of the Engle-Livine-Pereira-Rovelli spin foam model by a cosmological constant. Phys. Rev. D 97(8), 086010 (2018). http://arxiv.org/abs/1803.01838, arXiv:1803.01838 [gr-qc]

99. M. Assanioussi, B. Bahr, Hopf link volume simplicity constraints in spin foam models. Class. Quant. Grav. 37(20), 205003 (2020). http://arxiv.org/abs/2005.12004, arXiv:2005.12004 [gr-qc]

100. C. Allen, F. Girelli, S. Steinhaus, Numerical evaluation of spin foam amplitudes beyond simplices. Phys. Rev. D 105(6), 066003 (2022). http://arxiv.org/abs/2201.09902, arXiv:2201.09902 [gr-qc]

101. T. Hahn, CUBA: a library for multidimensional numerical integration. Comput. Phys. Commun. 168, 78-95 (2005). http://arxiv.org/abs/hep-ph/0404043, arXiv:hep-ph/0404043

102. B. Bahr, S. Steinhaus, Hypercuboidal renormalization in spin foam quantum gravity. Phys. Rev. D 95(12), 126006 (2017). http://arxiv.org/abs/1701.02311, arXiv:1701.02311 [gr-qc]

103. B. Bahr, G. Rabuffo, S. Steinhaus, Renormalization of symmetry restricted spin foam models with curvature in the asymptotic regime. Phys. Rev. D 98(10), 106026 (2018). http://arxiv.org/abs/1804.00023, arXiv:1804.00023 [gr-qc]

104. E. Bianchi, D. Regoli, C. Rovelli, Face amplitude of spinfoam quantum gravity. Class. Quant. Grav. 27, 185009 (2010). http://arxiv.org/abs/1005.0764, arXiv:1005.0764 [gr-qc]

105. H.W. Hamber, R.M. Williams, On the measure in simplicial gravity. Phys. Rev. D 59, 064014 (1999). http://arxiv.org/abs/hep-th/9708019, arXiv:hep-th/9708019

106. S. Steinhaus, J. Thürigen, Emergence of Spacetime in a restricted Spin-foam model. Phys. Rev. D 98(2), 026013 (2018). http://arxiv.org/abs/1803.10289, arXiv:1803.10289 [gr-qc]

107. M. Ali, S. Steinhaus, Towards "matter matters" in spin foam quantum gravity. http://arxiv.org/abs/2206.04076, arXiv:2206.04076 [gr-qc]

108. P. Dona, G. Sarno, Numerical methods for EPRL spin foam transition amplitudes and Lorentzian recoupling theory. Gen. Rel. Grav. 50, 127 (2018). http://arxiv.org/abs/1807.03066, arXiv:1807.03066 [gr-qc]

109. S.K. Asante, B. Dittrich, J. Padua-Arguelles, Effective spin foam models for Lorentzian quantum gravity. Class. Quant. Grav. 38(19), 195002 (2021). http://arxiv.org/abs/2104.00485, arXiv:2104.00485 [gr-qc]

110. B. Dittrich, A. Kogios, From spin foams to area metric dynamics to gravitons. http://arxiv.org/abs/2203.02409, arXiv:2203.02409 [gr-qc]

111. B. Dittrich, J.P. Ryan, Phase space descriptions for simplicial 4d geometries. Class. Quant. Grav. 28, 065006 (2011). http://arxiv.org/abs/0807.2806, arXiv:0807.2806 [gr-qc]

112. J.F.G. Barbero A real polynomial formulation of general relativity in terms of connections. Phys. Rev. D 49, 6935-6938 (1994). http://arxiv.org/abs/gr-qc/9311019, arXiv:gr-qc/9311019

113. G. Immirzi, The Reality conditions for the new canonical variables of general relativity. Class. Quant. Grav. 10, 2347-2352 (1993). http://arxiv.org/abs/hep-th/9202071, arXiv:hep-th/9202071

114. B. Dittrich, J.P. Ryan, On the role of the Barbero-Immirzi parameter in discrete quantum gravity. Class. Quant. Grav. 30, 095015 (2013). http://arxiv.org/abs/1209.4892arXiv:1209.4892 [gr-qc]

115. M. Christodoulou, M. Langvik, A. Riello, C. Roken, C. Rovelli, Divergences and orientation in spin-foams. Class. Quant. Grav. 30, 055009 (2013). http://arxiv.org/abs/1207.5156, arXiv:1207.5156 [gr-qc]

116. J. Engle, Proposed proper Engle-Pereira-Rovelli-Livine vertex amplitude. Phys. Rev. D 87(8), 084048 (2013). http://arxiv.org/abs/1111.2865, arXiv:1111.2865 [gr-qc]

117. A. Baratin, L. Freidel, A 2-categorical state sum model. J. Math. Phys. 56(1), 011705 (2015). http://arxiv.org/abs/1409.3526, arXiv:1409.3526 [math.QA]

118. A. Mikovic, M. Vojinovic, Poincare 2-group and quantum gravity. Class. Quant. Grav. 29, 165003 (2012). http://arxiv.org/abs/1110.4694, arXiv:1110.4694 [gr-qc]

119. S.K. Asante, B. Dittrich, F. Girelli, A. Riello, P. Tsimiklis, Quantum geometry from higher gauge theory. Class. Quant. Grav. 37(20), 205001 (2020). http://arxiv.org/abs/1908.05970, arXiv:1908.05970 [gr-qc]

120. L. Freidel, K. Krasnov, A new spin foam model for 4d gravity. Class. Quant. Grav. 25, 125018 (2008). http://arxiv.org/abs/0708.1595, arXiv:0708.1595 [gr-qc]

121. S.K. Asante, J.D. Simão, S. Steinhaus, Spin-foams as semi-classical vertices: gluing constraints and a hybrid algorithm. http://arxiv.org/abs/2206.13540, arXiv:2206.13540 [gr-qc]

122. V. Bonzom, Spin foam models for quantum gravity from lattice path integrals. Phys. Rev. D 80, 064028 (2009). http://arxiv.org/abs/0905.1501, arXiv:0905.1501 [gr-qc]

123. F. Hellmann, W. Kaminski, Holonomy spin foam models: asymptotic geometry of the partition function. JHEP 10, 165 (2013). http://arxiv.org/abs/1307.1679, arXiv:1307.1679 [gr-qc]

124. M. Han, M. Zhang, Asymptotics of spinfoam amplitude on simplicial manifold: Lorentzian theory. Class. Quant. Grav. 30, 165012 (2013). http://arxiv.org/abs/1109.0499, arXiv:1109.0499 [gr-qc]

125. J.S. Engle, W. Kaminski, J.R. Oliveira, Addendum to - EPRL/FK asymptotics and the flatness problem. [Addendum: Class. Quant. Grav. 38, 119401 (2021)]. http://arxiv.org/abs/2012.14822, arXiv:2012.14822 [gr-qc]

126. J.R. Oliveira, EPRL/FK asymptotics and the flatness problem. Class. Quant. Grav. 35(9), 095003 (2018). http://arxiv.org/abs/1704.04817, arXiv:1704.04817 [gr-qc]

127. P. Donà, F. Gozzini, G. Sarno, Numerical analysis of spin foam dynamics and the flatness problem. Phys. Rev. D 102(10), 106003 (2020). http://arxiv.org/abs/2004.12911, arXiv:2004.12911 [gr-qc]

128. M. Han, Semiclassical analysis of spinfoam model with a small Barbero-Immirzi parameter. Phys. Rev. D 88, 044051 (2013). http://arxiv.org/abs/1304.5628, arXiv:1304.5628 [gr-qc]

129. A. Ashtekar, J. Lewandowski, Quantum theory of geometry. I: area operators. Class. Quant. Grav. 14, A55-A82 (1997). http://arxiv.org/abs/gr-qc/9602046, arXiv:gr-qc/9602046

130. W. Wieland, Fock representation of gravitational boundary modes and the discreteness of the area spectrum. Ann. Henri Poincare 18(11), 3695-3717 (2017). http://arxiv.org/abs/1706.00479, arXiv:1706.00479 [gr-qc]

131. A. Ashtekar, J. Baez, A. Corichi, K. Krasnov, Quantum geometry and black hole entropy. Phys. Rev. Lett. 80, 904-907 (1998). http://arxiv.org/abs/gr-qc/9710007, arXiv:gr-qc/9710007

132. I. Agullo, J.F.G. Barbero, J. Diaz-Polo, E. Fernandez-Borja, E.J.S. Villasenor, Black hole state counting in LQG: a number theoretical approach. Phys. Rev. Lett. 100, 211301 (2008). http:// arxiv.org/abs/0802.4077, arXiv:0802.4077 [gr-qc]

133. J. Engle, K. Noui, A. Perez, D. Pranzetti, The SU(2) black hole entropy revisited. JHEP 05, 016 (2011). http://arxiv.org/abs/1103.2723, arXiv:1103.2723 [gr-qc]

134. J.F.G. Barbero, A. Perez, Quantum Geometry and Black Holes (WSP, 2017), pp. 241-279. http://dx.doi.org/10.1142/978 http://arxiv.org/abs/1501.02963, arXiv:1501.02963 [gr-qc]

135. B. Dittrich, Modified graviton dynamics from spin foams: the area Regge action. http://arxiv.org/abs/2105.10808, arXiv:2105.10808 [gr-qc]

136. F.P. Schuller, M.N.R. Wohlfarth, Geometry of manifolds with area metric: multi-metric backgrounds. Nucl. Phys. B 747, 398-422 (2006). http://arxiv.org/abs/hep-th/0508170, arXiv:hep-th/0508170

137. J.N. Borissova, B. Dittrich, Towards effective actions for the continuum limit of spin foams. http://arxiv.org/abs/2207.0 arXiv:2207.03307 [gr-qc]

138. K. Krasnov, Plebanski gravity without the simplicity constraints. Class. Quant. Grav. 26, 055002 (2009). http://arxiv.org/abs/0811.3147, arXiv:0811.3147 [gr-qc]

139. K. Krasnov, Gravity as BF theory plus potential. Int. J. Mod. Phys. A 24, 2776-2782 (2009). http://arxiv.org/abs/0907.4064, arXiv:0907.4064 [gr-qc]

140. W. Kaminski, M. Kisielowski, H. Sahlmann, Asymptotic analysis of the EPRL model with timelike tetrahedra. Class. Quant. Grav. 35(13), 135012 (2018). http://arxiv.org/abs/1705.02862, arXiv:1705.02862 [gr-qc]

141. H. Liu, M. Han, Asymptotic analysis of spin foam amplitude with timelike triangles. Phys. Rev. D 99(8), 084040 (2019). http://arxiv.org/abs/1810.09042, arXiv:1810.09042 [gr-qc]

142. J.D. Simão, S. Steinhaus, Asymptotic analysis of spin-foams with timelike faces in a new parametrization. Phys. Rev. D 104(12), 126001 (2021). http://arxiv.org/abs/2106.15635, arXiv:2106.15635 [gr-qc]

143. J. Ambjorn, J.L. Nielsen, J. Rolf, G.K. Savvidy, Spikes in quantum Regge calculus. Class. Quant. Grav. 14, 3225-3241 (1997). http://arxiv.org/abs/gr-qc/9704079, arXiv:gr-qc/9704079

144. C. Perini, C. Rovelli, S. Speziale, Self-energy and vertex radiative corrections in LQG. Phys. Lett. B 682, 78-84 (2009). http://arxiv.org/abs/0810.1714, arXiv:0810.1714 [gr-qc]

145. A. Riello, Self-energy of the Lorentzian Engle-Pereira-Rovelli-Livine and Freidel-Krasnov model of quantum gravity. Phys. Rev. D 88(2), 024011 (2013). http://arxiv.org/abs/1302.1781, arXiv:1302.1781 [gr-qc]

146. V. Bonzom, B. Dittrich, Bubble divergences and gauge symmetries in spin foams. Phys. Rev. D 88, 124021 (2013). http://arxiv.org/abs/1304.6632, arXiv:1304.6632 [gr-qc]

147. L.-Q. Chen, Bulk amplitude and degree of divergence in 4d spin foams. Phys. Rev. D 94(10) 104025 (2016). http://arxiv.org/abs/1602.01825, arXiv:1602.01825 [gr-qc]

148. P. Donà, Infrared divergences in the EPRL-FK Spin Foam model. Class. Quant. Grav. 35(17), 175019 (2018). http://arxiv.org/abs/1803.00835, arXiv:1803.00835 [gr-qc]